cells (Fig. S1). After cloning the PCR products, we sequenced all 43 clones obtained and compared the resulting sequences with that of mtDNA from P29 cells (Table 1). We found one and two somatic mutations in the mitochondrial $tRNA^{Leu(UUR)}$ and $tRNA^{Lys}$ genes, respectively. Given that each somatic mutation was present in only 1 of the 43 clones, the proportion of each in the mtDNA population of P29 cells would be about 2.2%.

The T7728C and G7731A mutations in the $tRNA^{Lys}$ gene both occurred in conserved sites (Table S1) and may correspond to pathogenic mutations that induce respiration defects by their accumulation. Moreover, an orthologous mutation to mouse G7731A has been reported to occur in human mtDNA from patients with mitochondrial diseases (10, 11).

Therefore, we selected these mutations in mtDNA for the generation of mito-mice. In an attempt to detect the T7728C and G7731A mutations in P29 mtDNA, we performed XmnI and DraI digestions of the PCR products of mtDNA, because the T7728C and G7731A mutations create an XmnI site and a DraI site, respectively (*SI Materials and Methods*). However, the T7728C and G7731A mutations were undetectable owing to their insufficient amounts in P29 cells.

Concentration of G7731A mtDNA in Subclones of P29 Cells. We previously showed that two mtDNA haplotypes with different mutations in single cells segregate stochastically during cell division (12). Therefore, some individual cells in the P29 population may possess detectable amounts of the mutated mtDNA. To obtain some individual cells that had accumulated either T7728C mtDNA or G7731A mtDNA from the P29 cell population, we isolated 100 subclones from P29 cells. Their mtDNA genotyping showed that two subclones, P29-42 and P29-69, possessed 34% and 48% G7731A mtDNA, respectively. However, we did not obtain any subclones carrying detectable amounts of T7728C mtDNA.

In the case of human mitochondrial *tRNA* gene mutations found in patients with mitochondrial diseases, respiration defects were apparent only when the mutated mtDNA had accumulated to more than 90% (13). To isolate P29 cells with more than 90% G7731A mtDNA, we cultured subclone P29-69, which had 48% G7731A mtDNA, for an additional 3 mo to allow further amplification of G7731A mtDNA through stochastic segregation; we then isolated more than 200 subclones from the P29-69 cells. We obtained one subclone, P29-69-183, which contained 92% G7731A mtDNA (Fig. 1*A*)—a level likely to be sufficient for the expression of respiration defects, if the G7731A mutation indeed is a pathogenic mutation.

Table 1. Somatic mutations in P29 mtDNA according to cloning and sequence analysis of the PCR products including the $tRNA^{Leu(UUR)}$ and $tRNA^{Lys}$ genes

	tRNA gene					
No. of clones	Leu^{UUR}	*Ile*	*Met*	Ser^{CUN}	*Lys*	*Lys*
Nucleotide position	2721	3760	3883	6931	7728*	7731†
P29 sequence‡	T	G	—	T	T	G
No. of clones						
1	del	—	—	—	—	—
1	—	A	—	—	—	—
1	—	—	insA	—	—	—
1	—	—	—	C	—	—
1	—	—	—	—	C	—
1	—	—	—	—	—	A
37	—	—	—	—	—	—

*The T7728C mutation in the $tRNA^{Lys}$ gene occurred in a site highly conserved throughout animals and fungi (Table 2). The mutation affects the first base of an anticodon triplet (TTT), resulting in an anticodon swap from TTT to CTT (Lys to Glu).

†The mutation equivalent to the G7731A mutation in the $tRNA^{Lys}$ gene of mice has been reported to occur in the mtDNA from human patients with mitochondrial diseases (10, 11).

‡Registered under GenBank accession no. EU312160.

Determination of the Pathogenicity of G7731A mtDNA. Comparison of the O_2 consumption rates between parental P29 cells and the P29-69-183 cells revealed the expression of respiration defects in the P29-69-183 cells (Fig. 1*B*). Moreover, P29-69-183 cells demonstrated slight overproduction of reactive oxygen species (Fig. 1*C*), indicating the pathogenicity of the G7731A mutation. Whole-sequence analysis of mtDNA in P29-69-183 cells showed that the G7731A mutation is the only mutation in those cells that is capable of inducing respiration defects (Table S2). However, we had to resolve two important issues before generation of the mito-mice carrying G7731A mtDNA.

First, we had to confirm that the respiration defects in P29-69-183 cells were due to G7731A mtDNA and not to the selection of cells with mutations in nuclear DNA that were acquired during repeated recloning. Second, P29-69-183 cells could not be used as mtDNA donors to isolate mouse ES cells with G7731A mtDNA

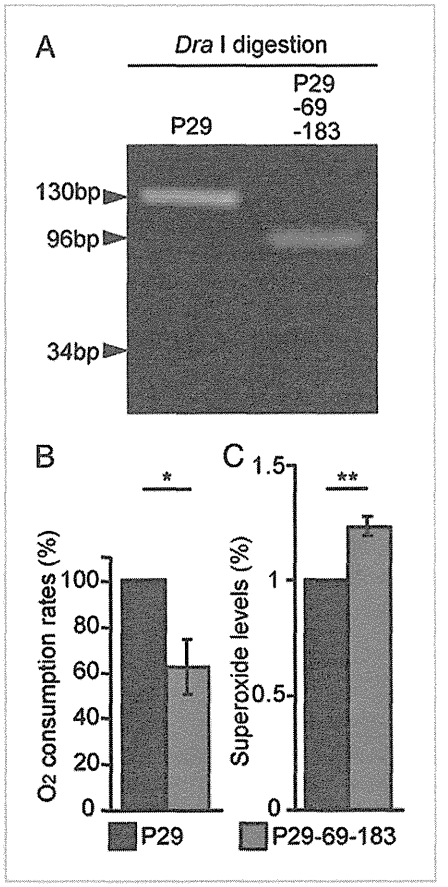

Fig. 1. Characterization of P29-69-183 cells to determine the pathogenicity of a G7731A mutation in the mitochondrial $tRNA^{Lys}$ gene. (*A*) Estimation of the proportion of G7731A mtDNA in P29 and P29-69-183 cells by DraI digestion of the PCR products. The G7731A mtDNA produced 96-bp and 34-bp fragments owing to the gain of a DraI site through G7731A substitution in the $tRNA^{Lys}$ gene, whereas mtDNA without the mutation produced a 130-bp fragment. Quantitative estimation of G7731A mtDNA showed that P29-69-183 cells contained 92% G7731A mtDNA. (*B*) Estimation of O_2 consumption rates of P29 and P29-69-183 cells. *$P < 0.05$. (*C*) Estimation of mitochondrial superoxide levels in P29 and P29-69-183 cells after their treatment with MitoSOX Red. **$P < 0.01$.

because of the difficulty of excluding unenucleated P29-69-183 cells from fusion mixtures of ES and enucleated P29-69-183 cells.

To simultaneously resolve these issues, we cytoplasmically transferred G7731A mtDNA from P29-69-183 cells into mtDNA-less (ρ^0) B82 cells (6). B82 cells are mouse fibrosarcoma cells that are resistant to BrdU and sensitive to hypoxanthine–aminopterin–thymidine (HAT) owing to their deficiency of thymidine kinase activity (6). Moreover, ρ^0 B82 cells are unable to grow in the absence of uridine and pyruvate owing to their complete lack of mtDNA. Using selection medium containing BrdU and lacking uridine and pyruvate, we isolated two colonies, B82mt7731-1 and B82mt7731-2. Genotyping of mtDNA showed that B82mt7731-1 and -2 possessed 70% and 95% G7731A mtDNA, respectively (Fig. 2*A*), indicating the transfer of G7731A mtDNA from P29-69-183 cells into ρ^0 B82 cells.

We then examined the respiratory function of these two cybrids by estimating O_2 consumption rates and the amounts of reactive oxygen species. The B82mt7731-2 cybrids showed decreased O_2 consumption rates (Fig. 2*B*) and increased production of reactive oxygen species (Fig. 2*C*) compared with those of B82mtB6 cybrids containing normal mtDNA from B6 mice. Therefore, respiration defects were transferred to B82mt7731 cybrids concurrently with the transfer of G7731A mtDNA from P29-69-183 cells into ρ^0 B82 cells, suggesting that the somatic G7731A mutation in mtDNA is a pathogenic mutation that can induce mitochondrial respiration defects by its predominant accumulation. Furthermore, B82mt7731 cybrids are effective as donors of G7731A mtDNA to ES cells, because unenucleated B82mt7731 cybrids can be excluded by using selection medium containing HAT.

Isolation of ES Cells Containing G7731A mtDNA and Their Chimeric Mice. Our previous study showed that no chimeric mice were obtained from ES cells carrying predominant amounts of ΔmtDNA, because the significant respiration defects induced by ΔmtDNA inhibited differentiation of ES cells to various tissues and germ cells (14). Therefore, we were concerned that the transfer of mtDNA from B82mt7731-2 cybrids containing 95% G7731A mtDNA to ES cells would inhibit generation of chimeric mice, and instead we used B82mt7731-1 cybrids containing lower proportions of G7731A mtDNA (Fig. 2*A*) as mtDNA donors.

Female (XO)-type ES cells (TT2 cells) were pretreated with rhodamine 6G (R6G) to eliminate endogenous mitochondria and mtDNA. They then were used as recipients of G7731A mtDNA and fused with enucleated B82mt7731-1 cybrids. The fusion mixture was cultured in selection medium containing HAT to exclude unenucleated B82mt7731-1 cybrids. Seven ES clones grew in the selective medium, two of which—clones ESmt7731-4 and ESmt7731-7—contained G7731A mtDNA (Fig. S2). The absence of G7731A mtDNA in the remaining five clones may be due to incomplete elimination of endogenous mtDNA in ES cells during R6G pretreatment.

We then aggregated the ESmt7731-4 and -7 cybrid clones with eight-cell-stage mouse embryos (ICR strain) and obtained 35 F_0 chimeric mice. Because mouse mtDNA is inherited strictly maternally (15, 16), we selected 15 F_0 chimeric female mice with 13–76% G13997A mtDNA in their tails as founder mice (Table 2) and mated them with B6 male mice to generate F_1 mice that carried G7731A mtDNA owing to its transfer through the female germ line.

Generation of Mito-Mice-tRNA^{Lys7731} via Female Germ-Line Transfer of G7731A mtDNA. Of the 15 F_0 female chimeras, 11 produced a total of 121 F_1 pups, 63 of which had G7731A mtDNA in their tails (Table 2). This finding suggests that G7731A mtDNA was transmitted maternally from F_0 female mice to F_1 progeny. Mice that carried G7731A mtDNA derived from lung carcinoma P29 cells were named "mito-mice-tRNA^{Lys7731}." Because the proportion of G7731A mtDNA did not differ significantly between tissues of the same F_1 male mito-mouse-tRNA^{Lys7731} (Fig. S3), we can deduce the approximate overall proportion of G7731A mtDNA in mito-mice-tRNA^{Lys7731} by estimating the proportion of G7731A mtDNA in the tail, which we can do without killing them.

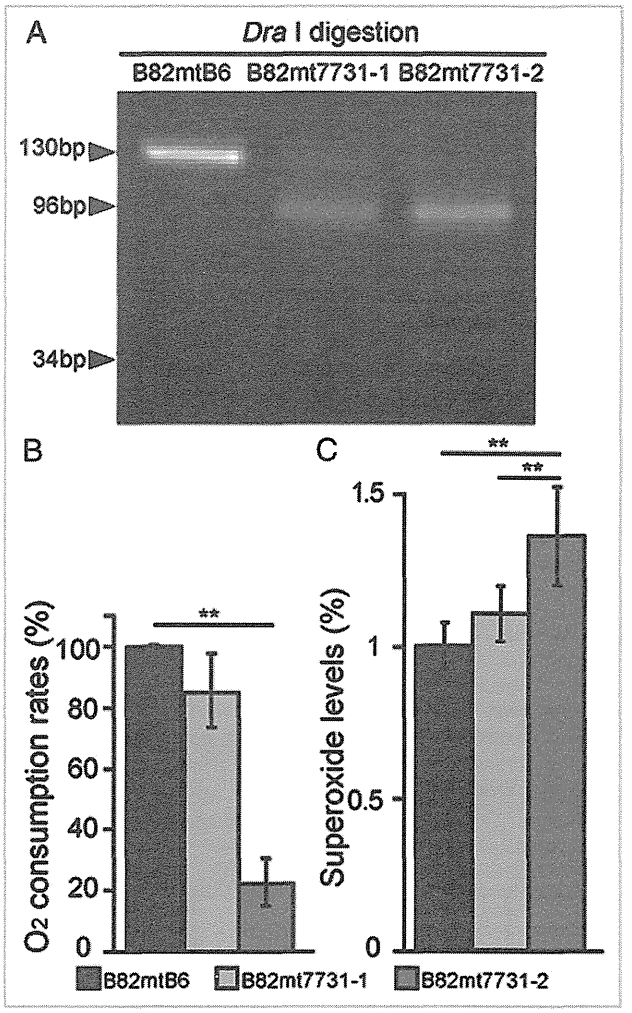

Fig. 2. Characterization of transmitochondrial B82mt7731 cybrids for their use as G7731A mtDNA donors to ES cells. (*A*) Estimation of the proportion of G7731A mtDNA in cybrids clones B82mt7731-1 and B82mt7731-2 by DraI digestion of the PCR products. Quantitative estimation of G7731A mtDNA showed that B82mt7731-1 and B82mt7731-2 had 70% and 95% G7731A mtDNA, respectively. (*B*) Estimation of O_2 consumption rates. $^{**}P < 0.01$. (*C*) Estimation of mitochondrial superoxide levels after treatment with Mito-SOX Red. $^{**}P < 0.01$.

Of the 63 F_1 mice with G7731A mtDNA in their tails, seven F_1 female mice carrying high proportions of G7731A mtDNA were mated with B6 male mice to obtain subsequent generations (F_2–F_5) of mito-mice-tRNA^{Lys7731} with sufficient G7731A mtDNA for the expression of respiration defects and resultant disorders. The proportions of G7731A mtDNA varied significantly among the pups born to each dam, but none of the pups carried more than 85% G7731A mtDNA (Fig. 3*A*).

To examine the reasons for the lack of mito-mice-tRNA^{Lys7731} with more than 85% G7731A mtDNA, we estimated the proportion of G7731A mtDNA in the oocytes obtained by ovarian hyperstimulation of F_5 female mito-mice-tRNA^{Lys7731} with high proportions of G7731A mtDNA. The results again showed significant variation in G7731A mtDNA proportions among the oocytes and the absence of oocytes with more than 85% G7731A mtDNA (Fig. 3*B*), indicating that lethality of oocytes with high

Table 2. Generation of F_0 chimeric mice and their F_1 progeny that carry G7731A mtDNA in their tails

		15 F_0 chimeric female mice		
ES clones	% G7731A mtDNA	% Chimerism*	% G7731A mtDNA in tails	No. of F_1 pups with G7731A mtDNA/no. of F_1 pups
ESmt7731-4	49.8	95	68	4/4
		95	53	2/12
		90	45	24/24
		50	48	0/17
		40	16	0/0
		35	21	0/8
ESmt7731-7	48.8	95	72	19/19
		95	76	4/4
		95	72	2/12
		95	68	8/8
		80	52	0/8
		60	61	0/5
		40	26	0/0
		15	13	0/0
		10	19	0/0
				Total: 63/121

*Chimerism was judged by coat color.

levels of G7731A mtDNA is responsible for the absence of mito-mice-tRNA^{Lys7731} carrying more than 85% G7731A mtDNA.

Expression of Disorders in Mito-Mice-tRNA^{Lys7731} with Predominant G7731A mtDNA. We used B6 mice as controls and three groups of F_5 mito-mice-tRNA^{Lys7731} with different heteroplasmic conditions (low, intermediate, and high levels of G7731A mtDNA) in their tails to examine various phenotypes relevant to mitochondrial diseases (Fig. 4).

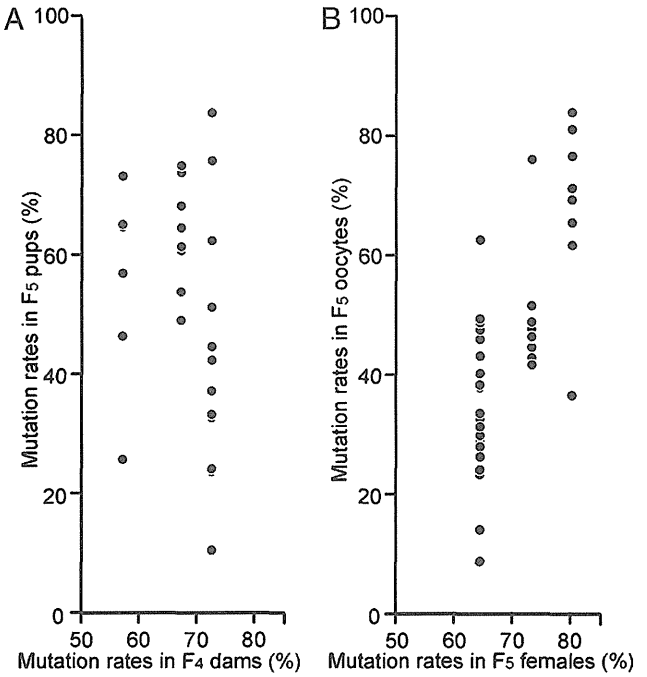

Fig. 3. Variation of G7731A mtDNA proportions among pups or oocytes from individual female mice. (*A*) Variation of G7731A mtDNA proportions among F_5 pups born to three F_4 dams. G7731A mtDNA proportions were estimated by using tails from F_5 pups that were obtained from three F_4 dams with high proportions of G7731A mtDNA. (*B*) Variation of G7731A mtDNA proportions among oocytes obtained from three F_5 female mice. G7731A mtDNA proportions were estimated by using oocytes obtained by ovarian hyperstimulation of F_5 female mito-mice-tRNA^{Lys7731} with high proportions of G7731A mtDNA.

First, we analyzed body length (Fig. 4*A*) and muscle strength (Fig. 4*B*), because abnormalities in these characteristics frequently occur in patients with mitochondrial diseases (10, 11), and these parameters can be examined without killing the mice. Unlike mito-mice tRNA^{Lys7731} with low and intermediate levels, those with high levels of G7731A mtDNA showed short body length (Fig. 4*A*) and muscle weakness (Fig. 4*B*), which are closely associated with the clinical phenotypes caused by mutations in the mitochondrial *tRNA^{Lys}* gene (2, 10, 11).

We then quantitatively estimated mitochondrial respiratory function and revealed respiration defects in skeletal muscle and kidney from mito-mice-tRNA^{Lys7731} with high levels of G7731A mtDNA (Fig. 4*C*). Therefore, accumulation of G7731A mtDNA likely is responsible for the respiration defects in mito-mice-tRNA^{Lys7731} with high levels of G7731A mtDNA (Fig. 4*C*). These respiration defects in the skeletal muscle subsequently result in the expression of muscle weakness (Fig. 4*B*), which corresponds to a phenotype relevant to mitochondrial diseases (2).

In contrast, other metabolic parameters relevant to mitochondrial diseases were normal (Fig. S4). Histochemical analysis showed that ragged-red fibers frequently observed in MERRF patients (2) and renal failures frequently observed in mito-mice-Δ (4, 5) were not found in mito-mice-tRNA^{Lys7731} (Figs. S5 and S6). Absence of these disorders in mito-mice-tRNA^{Lys7731} may be due in part to the fact that G7731A mtDNA proportions in the mice were not sufficient to induce significant respiration defects. For example, G8344A mtDNA proportions exceed 85% in patients with MERRF (2). Our failure to obtain mito-mice-tRNA^{Lys7731} with more than 85% G7731A mtDNA can be explained by the lethality of mouse oocytes carrying these levels of G7731A mtDNA (Fig. 3*B*).

These observations suggest that mito-mice-tRNA^{Lys7731} at least in part can serve as models to investigate pathogenesis of mitochondrial diseases that arise owing to mutations in the mitochondrial *tRNA* genes. In addition, the transmission profiles of G7731A mtDNA showed that selecting oocytes with lower levels of the mutated mtDNA likely would be effective to prevent maternal transmission of the disease phenotypes to the progeny.

Discussion

The current study generated mito-mice-tRNA^{Lys7731} carrying G7731A mtDNA with a pathogenic G7731A mutation in the mitochondrial *tRNA^{Lys}* gene. Specifically, we concentrated a small proportion of mtDNA with a somatic G7731A mutation

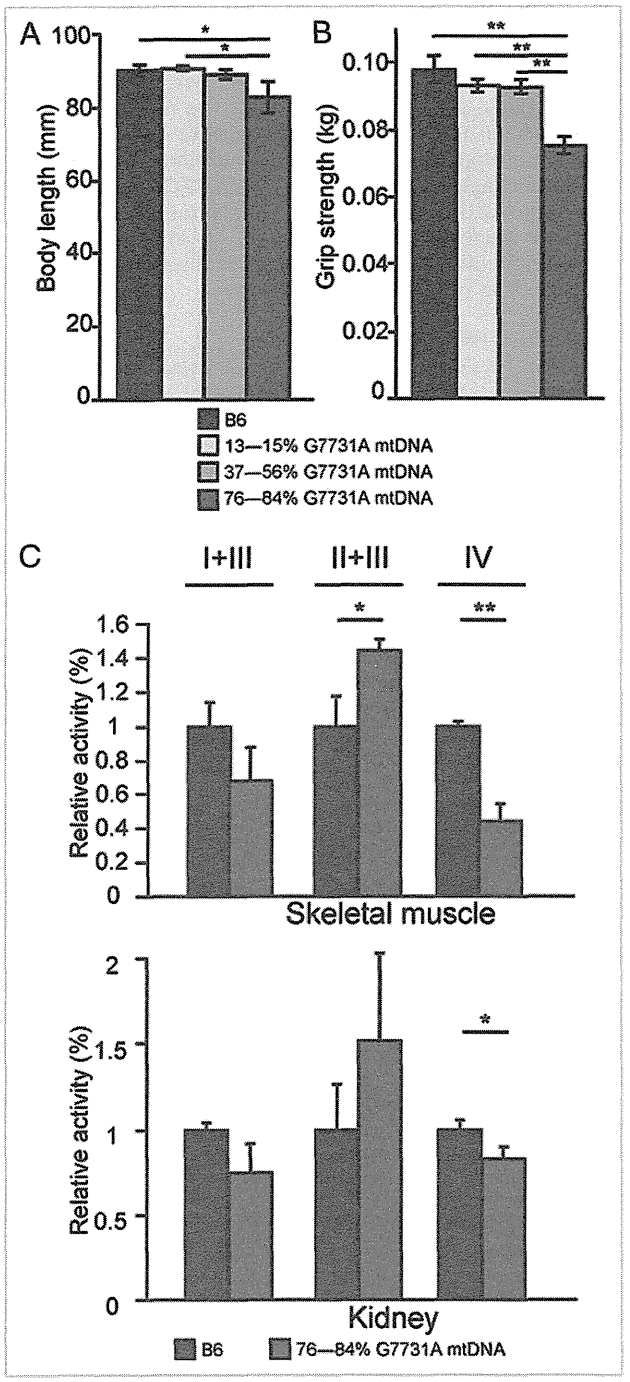

Fig. 4. Characterization of F_5 male mito-mice-tRNA^{Lys7731} according to phenotypes associated with mitochondrial diseases. Comparison of (*A*) body length and (*B*) muscle (grip) strength between B6 mice ($n = 3$) and F_5 mito-mice-tRNA^{Lys7731} carrying low (13–15%; $n = 3$), intermediate (37–56%; $n = 3$), and high (76–84%; $n = 3$) proportions of G7731A mtDNA. Body length and grip strength were measured at 4 mo after birth. Data are presented as means ± SD. $*P < 0.05$; $**P < 0.01$. (*C*) Comparison of activities of mitochondrial respiratory complexes (I + III, II + III, and IV) between B6 mice and F_5 mito-mice-tRNA^{Lys7731} carrying high proportions (76–84%) of G7731A mtDNA in the skeletal muscle and the kidney at 4 mo after birth. Respiratory complex I (NADH dehydrogenase), complex II (succinate dehydrogenase), complex III (cytochrome c reductase), and complex IV (cytochrome *c* oxidase) are components of the electron-transport chain. Enhanced activity of complex II + III in mito-mice-tRNA^{Lys7731} would be due to compensatory activation of complex II, which is controlled exclusively by nuclear DNA. Data are presented as means ± SD ($n = 3$). $*P < 0.05$; $**P < 0.01$.

that was present in P29 cells and then introduced it into ES cells to generate mito-mice-tRNA^{Lys7731}. The resulting mice were used to investigate the pathogenesis and transmission profiles of G7731A mtDNA.

Regarding the pathogenesis of G7731A mtDNA, mito-mice-tRNA^{Lys7731} with 74–84% G7731A mtDNA demonstrated respiration defects and the resultant muscle weakness and short body length (Fig. 4). These abnormalities in our mice are very similar to those found in patients with mitochondrial diseases owing to human orthologous G8328A mutation (10, 11) and in MERRF patients carrying the G8344A mutation in the *tRNA^{Lys}* gene (2, 17–19). Although these abnormalities were expressed in mito-mice-tRNA^{Lys7731} with 74–84% G7731A mtDNA (Fig. 4) and in the patients with 57% (10) and 82% G8328A mtDNA (11), more than 85% G8344A mtDNA was required for the onset of severe abnormalities in patients with MERRF (2, 17–19). However, we could not obtain mito-mice-tRNA^{Lys7731} with more than 85% G7731A mtDNA (Fig. 3*A*), which would be expected to induce significant respiration defects and severe abnormalities corresponding to MERRF, owing to the lethality of mouse oocytes with more than 85% G7731A mtDNA (Fig. 3*B*). Therefore, the expression of the significant respiration defects and severe clinical disorders in MERRF patients can be explained by supposing the absence of lethality in human oocytes even at G8344A mtDNA levels exceeding 85%. In contrast, our previous studies (4, 5) showed that mito-mice-Δ possessed more than 85% ΔmtDNA with a large-scale deletion and expressed significant respiration defects and severe abnormalities, even though their oocytes did not have more than 80% ΔmtDNA (20). The increase in the proportion of ΔmtDNA after birth may be due to its replication advantage (4, 5).

The absence of abnormalities in mito-mice-tRNA^{Lys7731} with intermediate levels (37–56%) of G7731A mtDNA (Fig. 4 *A* and *B*) seems to be different from what is observed for mtDNA with human orthologous G8328A mutation, because the patient with only 57% G8328A mtDNA in the skeletal muscles expressed disorders (10). This apparent discrepancy may be due to the aging effects in the patient with 57% G8328A mtDNA, considering that the phenotypes of the mito-mice-tRNA^{Lys7731} were examined 4 mo after birth (Fig. 4) and that the patient expressed disorders 45 y after birth (10). Thus, we have to examine whether mito-mice-tRNA^{Lys7731} with intermediate levels of G7731A mtDNA express abnormalities along with aging.

Regarding transmission profiles, those of mito-mice-tRNA^{Lys7731} are highly similar to those of MERRF patients, in that the mutated mtDNA is inherited by subsequent generations through the female germ line and the proportion of mutated mtDNA varied markedly among the pups born to each dam (Fig. 3*A*). The pups always carry wild-type mtDNA (Fig. 3*A*), owing to the significant pathogenicity of G7731A mtDNA and resultant induction of oocyte lethality in the absence of wild-type mtDNA (Fig. 3*B*). In contrast, we previously generated mito-mice-COI^{6589} (6) and mito-mice-ND6^{13997} (7, 8), which carry a 100% (homoplasmic) T6589C mtDNA mutation and a homoplasmic G13997A mtDNA mutation in the structural genes *COXI* and *ND6*, respectively, owing to the mild pathogenicity of the mutations. Because patients with MERRF and mito-mice-tRNA^{Lys7731} always carry both wild-type mtDNA and mutated mtDNA, mito-mice-tRNA^{Lys7731} are appropriate models for further investigating the transmission profiles of mutated mtDNA with marked pathogenicity.

The heteroplasmic mtDNA (wild-type mtDNA and mutated G7731A mtDNA) of our mito-mice-tRNA^{Lys7731} segregated stochastically, like those derived from different mouse strains (BALB and NZB) with polymorphic mutations (21) and those with and without point mutations (22). The significant variation in the G7731A mtDNA proportions among pups (Fig. 3*A*) may reflect "bottleneck effects" with (23, 24) or without decrease in the mtDNA copy number (25, 26) during female germ-line transmission of the heteroplasmic mtDNAs.

Regarding primary prevention of mitochondrial diseases, the results in Figs. 3 and 4 indicate that the selection of oocytes with

low proportions of G7731A mtDNA likely would yield phenotypically normal mice. In contrast, our previous study (20) showed that nuclear transplantation from zygotes of transmitochondrial mito-mice-Δ into enucleated zygotes with normal mtDNA is effective as germ-line gene therapy. Many recent reports similarly have noted that the use of the nuclear transplantation from human oocytes of affected mothers into enucleated oocytes donated by unrelated women would prevent the transmission of mitochondrial diseases caused by mtDNA mutations to their children (27–29). However, this technology includes the risk of inducing nuclear abnormalities, even though it excludes the risk of mitochondrial abnormalities. This problem would be resolved by the selection of oocytes with low proportions of mutated mtDNA. A previous study showed that polar bodies are effective for preimplantation genetic diagnosis (PGD) to deduce the proportion of mutated mtDNA in mouse oocytes (20). However, subsequent studies using polar bodies from human oocytes (30) and blastomeres from human embryos (31, 32) indicated that blastomeres are more appropriate than are polar bodies for PGD to deduce the proportion of mutated mtDNA. Although this procedure would not completely exclude the mutated mtDNA from the affected mothers, our previous studies (33, 34) showed the presence of intermitochondrial complementation to maintain normal respiratory function in the presence of the mutated mtDNA. Therefore, in light of the results in Figs. 3 and 4, we propose that the selection of embryos with low proportions of mutated mtDNA from affected mothers would be effective for obtaining unaffected children.

The risk of late-onset disorders in subjects with low proportions of mutated mtDNA seems to be negligible, because no subjects with less than 40% MERRF G8344A mutation in the blood expressed any abnormal symptoms throughout their lifetimes (17). Moreover, mito-mice-COI^{6589} carrying homoplasmic T6589C mtDNA in the *COX1* gene and expressing mild respiration defects showed normal lifespans and no late-onset disorders (6, 8). Although mito-mice-ND6^{13997} carrying homoplasmic G13997A mtDNA in the *ND6* gene developed late-onset and age-related disorders (8), the onset was not due to respiration defects but to overproduction of reactive oxygen species, which can be suppressed by the administration of antioxidants (8). Because high proportions of G7731A mtDNA also induced slight overproduction of reactive oxygen species (Fig. 2*C*), we will examine whether mito-mice-tRNA^{Lys7731} with high proportions of G7731A mtDNA express late-onset disorders owing to overproduction of reactive oxygen species.

Materials and Methods

Detailed information on materials and methods in this study is provided in *SI Materials and Methods*. Information on materials includes cell line and mice. Technical information on methods contains: cloning and sequencing of PCR products; genotyping of mtDNA; isolation of B82mt7731 and ESmt7731 cybrids; generation of chimeric mice and mitomice-tRNALys7731; oxygen consumption; measurement of reactive oxygen species in mitochondria; histopathological analyses; grip strength test; biochemical measurements of respiratory enzyme activity; measurement of blood glucose, lactate and blood urea nitrogen; measurement of hematocrit values; sequence analysis; and statistical analysis.

ACKNOWLEDGMENTS. This work was supported by Grants-in-Aid for Scientific Research A 25250011 (to J.-I.H.), Scientific Research A 23240058 (to K.N.), and Scientific Research on Innovative Areas 24117503 (to J.-I.H.) from the Japan Society for the Promotion of Science. This work was supported also by the World Premier International Research Center Initiative, Ministry of Education, Culture, Sports, Science and Technology–Japan (K.N. and J.-I.H.).

1. Larsson N-G, Clayton DA (1995) Molecular genetic aspects of human mitochondrial disorders. *Annu Rev Genet* 29:151–178.
2. Wallace DC (1999) Mitochondrial diseases in man and mouse. *Science* 283(5407): 1482–1488.
3. Taylor RW, Turnbull DM (2005) Mitochondrial DNA mutations in human disease. *Nat Rev Genet* 6(5):389–402.
4. Inoue K, et al. (2000) Generation of mice with mitochondrial dysfunction by introducing mouse mtDNA carrying a deletion into zygotes. *Nat Genet* 26(2):176–181.
5. Nakada K, et al. (2001) Inter-mitochondrial complementation: Mitochondria-specific system preventing mice from expression of disease phenotypes by mutant mtDNA. *Nat Med* 7(8):934–940.
6. Kasahara A, et al. (2006) Generation of trans-mitochondrial mice carrying homoplasmic mtDNAs with a missense mutation in a structural gene using ES cells. *Hum Mol Genet* 15(6):871–881.
7. Yokota M, et al. (2010) Generation of trans-mitochondrial mito-mice by the introduction of a pathogenic G13997A mtDNA from highly metastatic lung carcinoma cells. *FEBS Lett* 584(18):3943–3948.
8. Hashizume O, et al. (2012) Specific mitochondrial DNA mutation in mice regulates diabetes and lymphoma development. *Proc Natl Acad Sci USA* 109(26):10528–10533.
9. Ishikawa K, et al. (2008) ROS-generating mitochondrial DNA mutations can regulate tumor cell metastasis. *Science* 320(5876):661–664.
10. Houshmand M, Lindberg C, Moslemi AR, Oldfors A, Holme E (1999) A novel heteroplasmic point mutation in the mitochondrial tRNA(Lys) gene in a sporadic case of mitochondrial encephalomyopathy: De novo mutation and no transmission to the offspring. *Hum Mutat* 13(3):203–209.
11. Blakely EL, et al. (2007) Sporadic myopathy and exercise intolerance associated with the mitochondrial 8328G>A tRNALys mutation. *J Neurol* 254(9):1283–1285.
12. Hayashi J-I, Tagashira Y, Yoshida MC, Ajiro K, Sekiguchi T (1983) Two distinct types of mitochondrial DNA segregation in mouse-rat hybrid cells. Stochastic segregation and chromosome-dependent segregation. *Exp Cell Res* 147(1):51–61.
13. Chomyn A, et al. (1992) MELAS mutation in mtDNA binding site for transcription termination factor causes defects in protein synthesis and in respiration but no change in levels of upstream and downstream mature transcripts. *Proc Natl Acad Sci USA* 89(10):4221–4225.
14. Ishikawa K, et al. (2005) Application of ES cells for generation of respiration-deficient mice carrying mtDNA with a large-scale deletion. *Biochem Biophys Res Commun* 333(2):590–595.
15. Kaneda H, et al. (1995) Elimination of paternal mitochondrial DNA in intraspecific crosses during early mouse embryogenesis. *Proc Natl Acad Sci USA* 92(10):4542–4546.
16. Shitara H, Hayashi J-I, Takahama S, Kaneda H, Yonekawa H (1998) Maternal inheritance of mouse mtDNA in interspecific hybrids: Segregation of the leaked paternal mtDNA followed by the prevention of subsequent paternal leakage. *Genetics* 148(2):851–857.
17. Hammans SR, et al. (1993) The mitochondrial DNA transfer RNA^{Lys} A → G$^{(8344)}$ mutation and the syndrome of myoclonic epilepsy with ragged red fibres (MERRF). *Brain* 116(Pt 3):617–632.
18. Hammans SR, et al. (1995) The mitochondrial DNA transfer RNALeu(UUR) A—>G (3243) mutation. A clinical and genetic study. *Brain* 118(Pt 3):721–734.
19. Chinnery PF, Howell N, Lightowlers RN, Turnbull DM (1998) MELAS and MERRF. The relationship between maternal mutation load and the frequency of clinically affected offspring. *Brain* 121(Pt 10):1889–1894.
20. Sato A, et al. (2005) Gene therapy for progeny of mito-mice carrying pathogenic mtDNA by nuclear transplantation. *Proc Natl Acad Sci USA* 102(46):16765–16770.
21. Jenuth JP, Peterson AC, Fu K, Shoubridge EA (1996) Random genetic drift in the female germline explains the rapid segregation of mammalian mitochondrial DNA. *Nat Genet* 14(2):146–151.
22. Freyer C, et al. (2012) Variation in germline mtDNA heteroplasmy is determined prenatally but modified during subsequent transmission. *Nat Genet* 44(11):1282–1285.
23. Cree LM, et al. (2008) A reduction of mitochondrial DNA molecules during embryogenesis explains the rapid segregation of genotypes. *Nat Genet* 40(2):249–254.
24. Wai T, Teoli D, Shoubridge EA (2008) The mitochondrial DNA genetic bottleneck results from replication of a subpopulation of genomes. *Nat Genet* 40(12):1484–1488.
25. Cao L, et al. (2007) The mitochondrial bottleneck occurs without reduction of mtDNA content in female mouse germ cells. *Nat Genet* 39(3):386–390.
26. Cao L, et al. (2009) New evidence confirms that the mitochondrial bottleneck is generated without reduction of mitochondrial DNA content in early primordial germ cells of mice. *PLoS Genet* 5(12):e1000756.
27. Craven L, et al. (2010) Pronuclear transfer in human embryos to prevent transmission of mitochondrial DNA disease. *Nature* 465(7294):82–85.
28. Tachibana M, et al. (2013) Towards germline gene therapy of inherited mitochondrial diseases. *Nature* 493(7434):627–631.
29. Paull D, et al. (2013) Nuclear genome transfer in human oocytes eliminates mitochondrial DNA variants. *Nature* 493(7434):632–637.
30. Gigarel N, et al. (2011) Poor correlations in the levels of pathogenic mitochondrial DNA mutations in polar bodies versus oocytes and blastomeres in humans. *Am J Hum Genet* 88(4):494–498.
31. Steffann J, et al. (2006) Analysis of mtDNA variant segregation during early human embryonic development: a tool for successful NARP preimplantation diagnosis. *J Med Genet* 43(3):244–247.
32. Tajima H, et al. (2007) The development of novel quantification assay for mitochondrial DNA heteroplasmy aimed at preimplantation genetic diagnosis of Leigh encephalopathy. *J Assist Reprod Genet* 24(6):227–232.
33. Hayashi J-I, Takemitsu M, Goto Y-i, Nonaka I (1994) Human mitochondria and mitochondrial genome function as a single dynamic cellular unit. *J Cell Biol* 125(1):43–50.
34. Ono T, Isobe K, Nakada K, Hayashi J-I (2001) Human cells are protected from mitochondrial dysfunction by complementation of DNA products in fused mitochondria. *Nat Genet* 28(3):272–275.

Supporting Information

Shimizu et al. 10.1073/pnas.1318109111

SI Materials and Methods

Cell Lines and Cell Culture. Mouse P29 cells, their subclones, mtDNA-less (ρ^0) B82 cells, and their transmitochondrial cybrid clones were grown in DMEM (Sigma–Aldrich) containing 10% FCS, uridine (50 ng/mL), and pyruvate (100 ng/mL). Mouse ES cells (TT2-F, an XO subline established from XY TT2 cells; Riken BioResource Center) and transmitochondrial ES cybrids were cultivated on mitomycin-C–inactivated feeder cells derived from fetal fibroblasts in DMEM (Invitrogen) supplemented with 15% Knockout Serum Replacement (Invitrogen), nonessential amino acids (MP Biomedicals LLC), leukemia inhibitory factor (105 U/mL, Invitrogen), and 100 μM 2-mercaptoethanol (Sigma–Aldrich).

Cloning and Sequencing of PCR Products. Total DNA extracted from P29 cells was used as the template for PCR amplifications, which generated two mtDNA fragments, F1 and F2, by using unique primer pairs that were designed to generate 2.6- and 2.7-kb fragments, respectively. The sequences of the primers were based on the standard mtDNA sequence of B6 mice (GenBank accession no. AY172335): F1 forward, nucleotides 2045–2064; F1 reverse, 4623–4603; F2 forward, 5931–5950; and F2 reverse, 8626–8606 (Fig. S1). All PCR amplifications were performed in 50 μL of solution consisting of PCR buffer, 0.2 mM dNTPs, 0.6 mM primers, 1 U AmpliTaq Gold DNA polymerase (Perkin–Elmer Applied Biosystems), and 1 μg of cellular DNA as template. Reaction conditions were 95 °C for 10 min, followed by 35 cycles of 60 s at 95 °C, 60 s at 50–56 °C, and 150 s at 72 °C. PCR products were ligated into pUC118 (Takara) and then introduced into DH5α cells (Takara). Sequence templates were prepared by using a TempliPhi DNA Sequencing Template Amplification Kit (Amersham Pharmacia Biosciences) according to the manufacturer's protocol. Sequence reactions were performed by using dye termination methods (Takara PCR Thermal Cycler GP), and samples were sequenced on a MegaBACE1000 automated sequencer (Amersham Pharmacia Biosciences).

Genotyping of mtDNA. To detect the T7728C mutation, a 71-bp fragment containing the 7,728 site was PCR-amplified by using the nucleotide sequences 7703–7723 (5′-TATGAAGCTAAGAGCGgaAAC-3′; lowercase letters indicate mismatch) and 7773–7754 (5′-TGTGGCATATCACTATGGAG-3′) as oligonucleotide primers. Combination of the PCR-generated mutation with the T7728C mutation creates a restriction site for XmnI and generates 50- and 21-bp fragments on XmnI digestion of the PCR products. To detect the G7731A mutation, a 130-bp fragment containing the 7731 site was PCR-amplified by using the nucleotide sequences from 7633 to 7653 (5′-GCCCATTGTCCTAGAAATGGT-3′) and 7762–7732 (5′-ACTATGGAGATTTTAAGGTCTCTAACTTTAA-3′) as oligonucleotide primers. The G7731A mutation creates a restriction site for DraI and generates 96- and 34-bp fragments on DraI digestion of PCR products. The restriction fragments were separated by electrophoresis in a 3% (wt/vol) agarose gel. For quantification of G7731A mtDNA, we used the National Institutes of Health ImageJ program.

Isolation of B82mt7731 Cybrids. We used mtDNA-less (ρ^0) B82 cells as recipients for G7731A mtDNA. ρ^0 B82 cells are resistant to BrdU and sensitive to hypoxanthine–aminopterin–thymidine (HAT) owing to their deficiency of thymidine kinase activity. Furthermore, ρ^0 B82 cells are unable to grow in the absence of uridine and pyruvate owing to their absence of mtDNA. mtDNA donor P29-69-183 cells were pretreated with cytochalasin B (10 μg/mL) for 10 min and centrifuged at 7,500 × *g* for 10 min at 37 °C for enucleation; the resultant cytoplasts were fused with ρ^0 B82 cells by using polyethylene glycol. The fusion mixture was cultured in selection medium containing BrdU (30 μg/mL) and lacking uridine and pyruvate. The selection medium excluded unenucleated P29-69-183 cells and unfused ρ^0 B82 and thus allowed exclusive growth of transmitochondrial B82mt7731 cybrids.

Isolation of ESmt7731 Cybrids. Host ES cells were pretreated with rhodamine 6G (R6G; 0.38–1.5 μg/mL in 3% (wt/vol) ethanol) for 48 h to eliminate endogenous mitochondria and mtDNA (1, 2). The ES cells then were washed with PBS and suspended in R6G-free medium for 2 h to allow recovery. mtDNA donor B82mt7731 cybrids were pretreated with cytochalasin B (10 μg/mL) for 10 min and centrifuged at 22,500 × *g* for 30 min at 37 °C for enucleation. The resultant cytoplasts were fused with R6G-pretreated ES cells by using polyethylene glycol, and the fusion mixture was cultured in selection medium containing HAT to exclude unenucleated B82mt7731 cybrids. At 7 d after fusion, growing colonies were harvested for mtDNA genotyping. Under these selection conditions, ES cells containing recovered endogenous mtDNA were not eliminated completely, owing to insufficient R6G treatment.

Generation of Chimeric Mice and Mito-Mice-tRNA^{Lys7731}. Frozen eight-cell-stage embryos of ICR mice (ARK Resource Company) were thawed and their zona pellucidae were removed by treatment with acidified Tyrode's buffer (Sigma–Aldrich). Each treated embryo was placed with about 50 ESmt7731 cybrids in a well of a 35-mm culture dish and incubated overnight to enable aggregation. The next day, the embryos were transferred into pseudopregnant ICR female mice (Japan SLC). The resulting progeny were identified by their coat-color chimerism. Founder (F_0) chimeric female mice were mated with C57BL/6 J (B6; CLEA Japan) male mice to produce the F_1 generation, and F_1 female mice with G7731A mtDNA in their tails (F_1 female mito-mice-tRNA^{Lys7731}) were back-crossed with B6 male mice to obtain F_2 mito-mice-tRNA^{Lys7731}.

Mice. Inbred B6 mice generated through more than 40 rounds of brother–sister mating were obtained from CLEA Japan. We maintained mito-mice-tRNA^{Lys7731} by repeated back-crossing of these female mice with B6 male mice. Animal experiments were performed in accordance with protocols approved by the Experimental Animal Committee of the University of Tsukuba (approval number 12070).

Oxygen Consumption. Cells were washed once in PBS and then resuspended in PBS at a density of 4 × 10^6 cells/mL. Oxygen consumption was measured by using an oxygraph equipped with a Clark-type electrode (model 5300; Yellow Springs Instruments Company) at 37 °C. The cell suspension (2 mL) was transferred to a polarographic cell, and basal respiration was measured immediately under constant stirring.

Measurement of Reactive Oxygen Species in Mitochondria. Reactive oxygen species were detected by using the mitochondrial superoxide indicator MitoSOX Red (Invitrogen). Cells were incubated with 1 mM MitoSOX Red for 15 min at 37 °C in PBS, washed twice with PBS, and then immediately analyzed by using flow cytometry (FACScan; Becton Dickinson).

Histopathologic Analyses. Formalin-fixed, paraffin-embedded sections (5-μm thickness) were stained with hematoxylin and eosin to identify cases of renal failure. Cryosections (10-μm thickness) of skeletal muscle were stained by using a modified Gomori trichrome to identify ragged-red fibers (RRFs).

Grip Strength Test. Muscle strength was estimated by using a Grip Strength Meter (Columbus Instruments); three sequential trials were performed on each mouse.

Biochemical Measurements of Respiratory Enzyme Activity. Mitochondrial respiratory complex I (NADH dehydrogenase), complex II (succinate dehydrogenase), and complex III (cytochrome c reductase) are components of the electron-transport chain and are located in the mitochondrial inner membrane. The activity of these enzymes was assayed as described previously (3). Briefly, to estimate the activity owing to complex I + III, NADH and cytochrome c (oxidized form) were used as substrates, and the reduction in cytochrome c was monitored by measuring absorbance at a wavelength of 550 nm. To estimate the activity owing to complex II + III, sodium succinate and cytochrome c (oxidized form) were used as substrates, and the reduction of cytochrome c was monitored as described previously.

Measurement of Blood Glucose, Lactate, and Blood Urea Nitrogen. To determine fasting blood lactate and glucose concentrations, peripheral blood was collected from the tail veins of mice after overnight fasting from food. After oral administration of glucose (1.5 g/kg body weight), blood was collected again, and lactate and glucose concentrations were measured by using an automatic blood lactate test meter (Lactate Pro; Arkray) and glucose test meter (Dexter ZII; Bayer), respectively. Blood urea nitrogen was measured by using a Urea N B test (Wako Pure Chemical) in accordance with the manufacturer's protocol.

Measurement of Hematocrit Values. To determine hematocrit levels, capillary blood was collected from each mouse into heparinized capillary tubes and centrifuged at 10,500 × *g* for 5 min. Packed cell volumes were measured by using a hematocrit reader.

Sequence Analysis. Each DNA (3 μg) extracted from P29-69-183 cells and from kidney of mito-mouse-tRNA^{Lys7731} were used to prepare the sequencing libraries. These sequencing libraries were constructed by using the TruSeq DNA LT Sample Prep Kit (Illumina) according to the instructions in "TruSeq DNA Sample Preparation Guide Rev. C" (Illumina). These sample DNAs were sheared by using an acoustic solubilizer (Covaris), and the overhangs resulting from the fragmentation were converted to blunt ends by phosphorylation of the DNA fragments. The blunt fragments were adenylated at their 3′ ends and were ligated to the ends of the DNA fragments, which were subsequently enriched by PCR. Clonal template clusters were generated from the sequencing library, and sequencing was performed by the reversible terminator-based method (4). Base calling and data conversion into Fastq files were performed by using software providing the Burrows–Wheeler Alignment Tool (5).

Statistical Analysis. Data are presented as means ± SD and were analyzed by using Student *t* test; *P* values less than 0.05 were considered significant.

1. Ziegler ML, Davidson RL (1981) Elimination of mitochondrial elements and improved viability in hybrid cells. *Somatic Cell Genet* 7(1):73–88.
2. McKenzie M, Trounce IA, Cassar CA, Pinkert CA (2004) Production of homoplasmic xenomitochondrial mice. *Proc Natl Acad Sci USA* 101(6):1685–1690.
3. Miyabayashi S, et al. (1989) Defective pattern of mitochondrial respiratory enzymes in mitochondrial myopathy. *J Inherit Metab Dis* 12(3):373–377.
4. Bentley DR, et al. (2008) Accurate whole human genome sequencing using reversible terminator chemistry. *Nature* 456(7218):53–59.
5. Li H, Durbin R (2009) Fast and accurate short read alignment with Burrows-Wheeler transform. *Bioinformatics* 25(14):1754–1760.

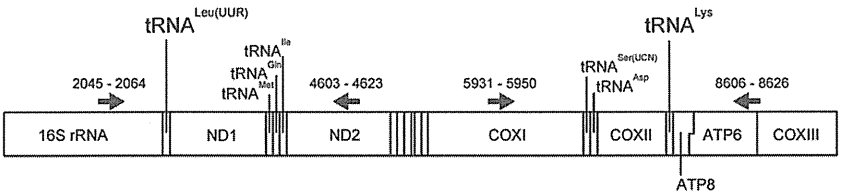

Fig. S1. Nucleotide positions of PCR primers on the mouse mtDNA map. To detect small proportions of mtDNA with somatic but possibly pathogenic mutations in the *tRNA*$^{Leu(UUR)}$ and *tRNA*^{Lys} genes of P29 cells, we used two sets of PCR primers so that the resultant PCR products included the *tRNA*$^{Leu(UUR)}$ and *tRNA*^{Lys} genes, respectively. These products also included five additional *tRNA* genes (*tRNA*^{Ile}, *tRNA*^{Gln}, *tRNA*^{Met}, *tRNA*$^{Ser(CUN)}$, and *tRNA*^{Asp}).

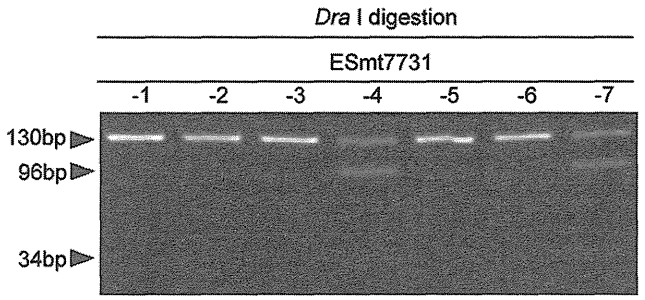

Fig. S2. Identification of G7731A mtDNA in ESmt7731 cybrid clones grown in selection medium. We were able to obtain two ESmt7731 cybrid clones carrying G7731A mtDNA (ESmt7731-4 and ESmt7731-7) but were unable to exclude ES cells that lacked G7731A mtDNA, owing to incomplete elimination of endogenous mtDNA by R6G treatment. Accordingly, ESmt7731-1, -2, -3, -5, and -6 correspond to ES cells that lacked G7731A mtDNA but contained endogenous mtDNA.

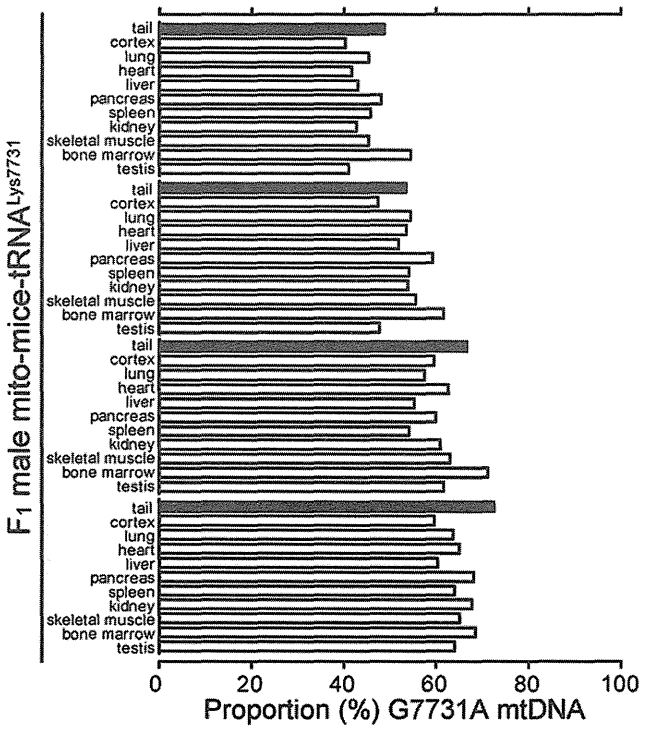

Fig. S3. Proportions of G7731A mtDNA in the tissues from a single F_1 male mouse. Note that the proportion of G7731A mtDNA did not differ significantly among different tissues from the same F_1 male mito-mice-tRNA^{Lys7731}, suggesting that we can deduce the overall proportion of G7731A mtDNA in mito-mice-tRNA^{Lys7731} from that in the tail without killing the mice.

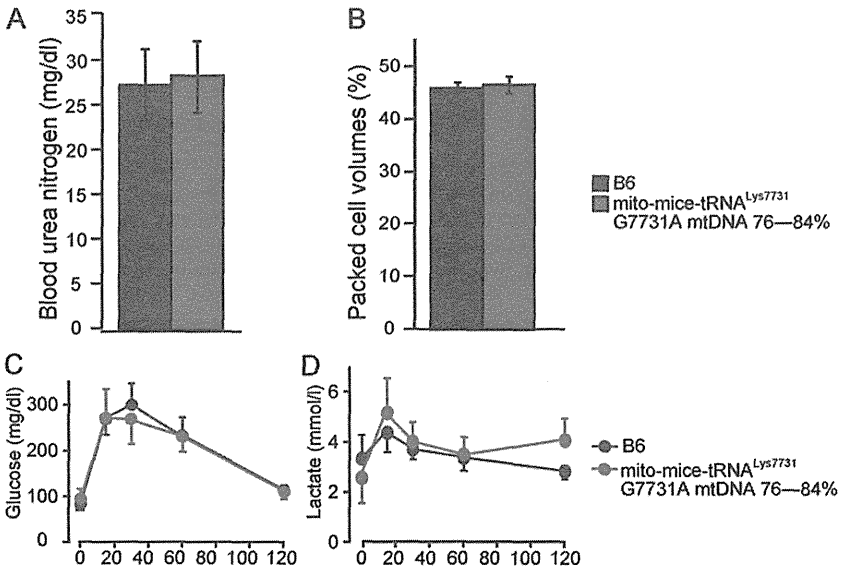

Fig. S4. Analyses of metabolic parameters related to mitochondrial diseases by using peripheral blood from mito-mice-tRNA^{Lys7731} with high proportions of G7731A mtDNA. (*A*) Blood urea nitrogen. (*B*) Hematocrit. (*C*) Blood glucose levels before and after glucose administration. (*D*) Blood lactate levels before and after glucose administration. No statistically significant differences between B6 and mito-mice-tRNA^{Lys7731} with high proportions of G7731A mtDNA were obtained. Data are presented as mean ± SD (n = 3).

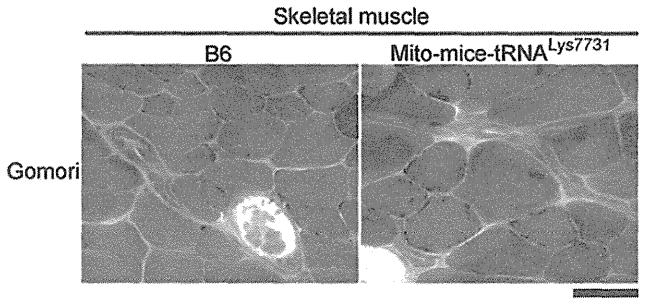

Fig. S5. Histopathologic analysis to identify RRFs in skeletal muscle. Cryosections (10-μm thickness) of skeletal muscle were stained by using modified Gomori trichrome for histopathologic analysis to identify RRF. No RRFs were present in mito-mice-tRNA^{Lys7731} with high proportions of G7731A mtDNA. (Scale bar, 50 μm.)

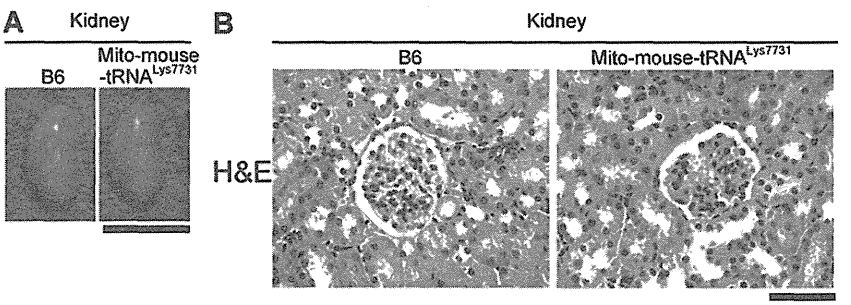

Fig. S6. Morphology and histopathologic analysis of kidney. (*A*) Morphology of kidneys from B6 mice (*Left*) and mito-mice-tRNA^{Lys7731} with 76% G7731A mtDNA (*Right*). (Scale bar, 1 cm.) (*B*) Histopathology of the renal cortex of kidneys from B6 mice (*Left*) and mito-mice-tRNA^{Lys7731} with 76% G7731A mtDNA (*Right*). Formalin-fixed, paraffin-embedded sections (5-μm thickness) were stained with hematoxylin and eosin. No renal failure was noted in mito-mice-tRNA^{Lys7731}. (Scale bar, 50 μm.)

Table S1. Comparison of mutations in the mouse mitochondrial *tRNA* gene with the wild-type *tRNA* genes of other species

	Leu(UUR)	*Lys*	
	del2721T	T7728C	G7731A
Mutation	–	C	A
Mouse	T	T	G
Human	C	T	G
Xenopus	T	T	G
Zebrafish	C	T	G
Drosophila	T	T	A
Nematoda	–	T	T
Yeast	C	T	G

The GenBank accession nos. of the sequences used in the alignment are mouse, AY172335; human, NC_012920; *Xenopus*, NC_001573; zebrafish, NC_002333; *Drosophila*, NC001709; Nematoda, NC_001328; and yeast, NC_001224.

Table S2. Whole-sequence analysis of the mtDNA from P29-69-183 cells and mito-mice-tRNA^{Lys7731}

	Genes					
	tRNA^{Lys}		*tRNA^{Arg}*		D-loop	
Nucleotide position	7731	9818~	9821~		16099	16105
P29 sequence*	G	$(T)_3$	$(A)_9$	$(A)_9$	A	T
Variant sequence	A	$(T)_2$	$(A)_8$	$(A)_{10}$	C	C
P29-69-183*	89.6%†	16.4%	8.2%	6.5%	31.6%	47.6%
Mito-mouse-tRNA^{Lys7731}‡	80.0%	3.6%	0.5%	18.1%	26.9%	37.0%

*Registered under GenBank accession nos. EU312160 (for P29) and AP014540 (for P29-69-183).
†Whole-sequence analysis of mtDNA from P29-69-183 cells showed that they had 89.6% G7731A mtDNA. This value was almost equivalent to that obtained in Fig. 1*A* (92%), suggesting the reliability of our quantification of G7731A mtDNA proportion by using restriction fragment length polymorphism.
‡Kidney of F_5 mito-mouse-tRNA^{Lys7731} possessing 81.3% G7731A mtDNA quantified by using restriction fragment length polymorphism was used for whole-sequence analysis of the mtDNA. All polymorphic mutations found in mtDNA of P29-69-183 cells have persisted in mtDNA of a mito-mouse-tRNA^{Lys7731}.

Mitochondrion 20 (2015) 34–42

Contents lists available at ScienceDirect

Mitochondrion

journal homepage: www.elsevier.com/locate/mito

GDF15 is a novel biomarker to evaluate efficacy of pyruvate therapy for mitochondrial diseases

Yasunori Fujita [a], Masafumi Ito [a], Toshio Kojima [b], Shuichi Yatsuga [c], Yasutoshi Koga [c], Masashi Tanaka [d,*]

[a] Research Team for Mechanism of Aging, Tokyo Metropolitan Institute of Gerontology, 35-2 Sakae-cho, Itabashi, Tokyo 173-0015, Japan
[b] Health Support Center, Toyohashi University of Technology, 1-1 Hibarigaoka Tenpaku-cho, Toyohashi, Aichi 441-8580, Japan
[c] Department of Pediatrics and Child Health, Kurume University School of Medicine, 67 Asahi-machi, Kurume, Fukuoka 830-0011, Japan
[d] Department of Genomics for Longevity and Health, Tokyo Metropolitan Institute of Gerontology, 35-2 Sakae-cho, Itabashi, Tokyo 173-0015, Japan

ARTICLE INFO

Article history:
Received 20 May 2014
received in revised form 2 September 2014
accepted 29 October 2014
Available online 1 November 2014

Keywords:
GDF15
Pyruvate
Mitochondrial diseases
Cybrid
Microarray
Biomarker

ABSTRACT

Pyruvate therapy is a promising approach for the treatment of mitochondrial diseases. To identify novel biomarkers for diagnosis and to evaluate therapeutic efficacy, we performed microarray analysis of 2SD cybrid cells harboring a MELAS-causing mutation and control cells treated with either lactate or pyruvate. We found that expression and secretion of growth differentiation factor 15 (GDF15) were increased in 2SD cells treated with lactate and that serum GDF15 levels were significantly higher in patients with mitochondrial diseases than in those with other diseases, suggesting that GDF15 could be a useful marker for diagnosis and evaluating the therapeutic efficacy of pyruvate.

1. Introduction

Mitochondrial diseases are caused by mitochondrial or nuclear genome mutations that affect the functions of mitochondria. The symptoms are caused by impaired energy metabolism due to mitochondrial dysfunction and manifest mostly in tissues with a high energy demand such as brain, heart, and muscle. Mitochondrial myopathy, encephalopathy, lactic acidosis, and stroke-like episodes (MELAS) is one of the most common of the mitochondrial diseases (Pavlakis et al., 1984). The A-to-G transition at the 3243 position of the mitochondrial DNA (m.3243A > G) located in the mitochondrial $tRNA^{Leu\ (UUR)}$ gene is a MELAS-causing mutation, and it is detected in approximately 80% of patients with MELAS (Goto et al., 1990, 1992; Kirino et al., 2004; Yasukawa et al., 2000).

These pathogenic mutations typically result in defective ATP synthesis in mitochondria, and therefore ATP production depends on the glycolytic pathway. Since lactate production is aberrantly increased by the acceleration of glycolysis when energy demand is elevated, the lactate to pyruvate (L/P) ratio in serum is often increased in patients with mitochondrial diseases and has been clinically used for estimating the dysfunction of mitochondrial respiration. It is well known that the L/P ratio reflects the intracellular NADH/NAD^+ ratio. Since NAD^+ is indispensable for oxidation of glyceraldehyde 3-phosphate (GAP) to 1,3-bisphosphoglycerate (BPG) by glyceraldehyde 3-phosphate dehydrogenase (GAPDH) in the glycolytic pathway, a shortage of NAD^+ interrupts this reaction, resulting in decreased ATP biosynthesis. Tanaka et al. (2007) proposed that the addition of pyruvate would facilitate oxidation of NADH to NAD^+ via the lactate dehydrogenase reaction, which would restore ATP production by the glycolytic pathway even under defective respiratory conditions. Indeed, positive effects of sodium pyruvate on clinical manifestations of mitochondrial diseases have been reported (Koga et al., 2012; Saito et al., 2012). However, useful biomarkers for evaluating the therapeutic efficacy of pyruvate remain to be developed.

Cybrid cell lines established by the fusion of enucleated myoblast cells from a patient with a cultured cell line depleted of mtDNA have been used to elucidate the pathogenesis and underlying molecular mechanisms of mitochondrial diseases. We previously reported increased expression of amino acid starvation-responsive genes in cybrid cells with MELAS and NARP (neuropathy, ataxia, and retinitis pigmentosa) mutations (Fujita et al., 2007). In our earlier study (Kami et al., 2012), we found that exposure to excessive sodium lactate significantly increases the intracellular L/P and NADH/NAD^+ ratios in cybrid cells harboring the MELAS mutation (m.3243A > G), which implies worsening of lactic acidosis and NAD^+ shortage. On the other hand, we found that treatment with sodium pyruvate facilitates the ATP production and improves the energy status, as indicated by a decrease in the L/P ratio and retention of the NADH/NAD^+ ratio. Taken together, we considered that these experimental conditions would be ideal for identifying biomarker candidate genes, whose expression levels reflect

* Corresponding author. Tel.: +81 3 3964 3241; fax: +81 3 3579 4776.
E-mail address: mtanaka@tmig.or.jp (M. Tanaka).

http://dx.doi.org/10.1016/j.mito.2014.10.006
1567-7249/

the intracellular energy deficiency and the effect of pyruvate on energy metabolism.

In the present study, we performed a global gene expression analysis of cybrid cells with the MELAS mutation (m.3243A > G: 2SD cells) and control cybrid cells (2SA cells) treated or not with lactate or pyruvate. We identified several biomarker candidate genes, among which we focused on growth differentiation factor 15 (GDF15). The level of GDF15 in the conditioned medium was significantly higher in 2SD cells than in 2SA cells, which level was further increased by lactate but was not affected by pyruvate in 2SD cells. We also demonstrated that the concentration of GDF15 in the serum was markedly elevated in patients with mitochondrial diseases compared with that in those with other pediatric diseases. Thus, we identified GDF15 as a novel serum marker for the diagnosis of mitochondrial diseases and possibly for monitoring the disease status and progression and for evaluating the therapeutic efficacy of pyruvate.

2. Materials and methods

2.1. Cell culture

The 2SA and 2SD cybrid cell lines were previously established by Chomyn et al. (1992). Briefly, 14 cybrid clones were isolated after the fusion of enucleated myoblasts derived from a MELAS patient with mtDNA-deficient $\rho^0$206 cells generated from a human 143B osteosarcoma cell line. Among those clones, 10 clones had homoplasmic wild-type mtDNA, and 4 clones harbored strongly predominant mutant mtDNA. For our experiments, we chose two clones, 2SA and 2SD cybrid cell lines carrying 100% wild-type mtDNA and 94% m.3243A > G mutant mtDNA, respectively. The 2SD but not 2SA cybrid cells were shown to be defective in mitochondrial protein synthesis and respiratory capacity (Chomyn et al., 1992). Cells were cultured in high-glucose Dulbecco's modified Eagle's medium (DMEM) supplemented with 10% fetal bovine serum, 1 mM sodium pyruvate, and 0.4 mM uridine at 37 °C under a humidified atmosphere of 5% CO_2.

2.2. Microarray analysis

Total RNA was isolated from cells by using a miRNeasy mini kit (Qiagen, Venlo, Netherlands). One hundred nanograms of total RNA was labeled and amplified with a low input quick amp labeling kit (Agilent Technologies, Santa Clara, CA, USA) used according to the manufacturer's instructions. The labeled cRNA was hybridized to the Agilent SurePrint G3 Human GE 8x60K Microarray in a rotating hybridization oven at 10 rpm for 20 h at 65 °C. After hybridization, the microarrays were washed according to the manufacturer's instructions and scanned on an Agilent DNA Microarray Scanner with Scan Control software. The resulting images were processed, and raw data were collected by using Agilent Feature Extraction software. Expression data were analyzed by using GeneSpring GX 11 (Agilent Technologies). The signal intensity of each probe was normalized by a percentile shift, in which each value was divided by the 75th percentile of all values in its array. For pairwise comparison analysis, only the probes that had expression flags present under at least one condition were considered. The list was analyzed with Ingenuity Pathways Analysis software (Ingenuity Systems, Redwood, CA, USA)

2.3. Quantitative RT-PCR

Total RNA was reverse transcribed to cDNA with a High Capacity cDNA Reverse Transcription Kit (Life Technologies, Carlsbad, CA, USA) used according to the manufacturer's protocols. Real-time PCR was performed on the StepOnePlus Real-Time PCR System (Life Technologies) using Power SYBR Green PCR Master Mix. 18S rRNA gene was used as an internal control for normalization. The sequences of primers are listed in Supplementary Table 1.

2.4. Patients

A written informed consent was obtained from all patients or their legal guardians. Enrolled patients were diagnosed with mitochondrial diseases by medical doctors in Kurume University Hospital over the period of 2005–2013. Seventeen patients diagnosed at this hospital as having mitochondrial diseases were recruited for this study. As a control group, 13 patients diagnosed as having other pediatric diseases such as dwarfism were also recruited. The clinical information of the patients is listed in Supplementary Table 2. This study was approved by the Institutional Review Board (Kurume University #13099).

2.5. ELISA and multiplex suspension array

Cells were placed on 60-mm dishes 1 day before replacing the medium with fresh medium. Conditioned medium cultured for 24 h was collected, and the particulates were removed by centrifugation (at 500 ×*g* for 10 min, at 10,000 ×*g* for 30 min). The GDF15 and INHBE concentrations in the supernatants and in the sera of patients were determined in duplicate by using a Human GDF-15 Immunoassay (R&D Systems, Minneapolis, MN, USA) and enzyme-linked immunosorbent assay kit for Inhibin Beta E (Uscn Life Science, Wuhan, Hubei, PRC) according to the manufacturer's instructions. For measuring other cytokine concentrations, the sera were subjected to a multiplex suspension array, Bio-Plex Pro Human Cytokine Grp II Panel 21-Plex (Bio-Rad, Hercules, CA, USA). The cytokines measured by use of this array were the following: IL-1α, IL-2Rα, IL-3, IL-12 (p40), IL-16, IL-18, CTACK, GRO-α, HGF, IFN-α2, LIF, MCP-3, M-CSF, MIF, MIG, β-NGF, SCF, SCGF-β, SDF-1α, TNF-β, and TRAIL. We measured the FGF21 (BioVendor, Czech Republic) concentration in duplicate samples by ELISA. Unmeasurable high-concentration samples of FGF21 and GDF15 were diluted 10-fold prior to measurement. The value from each assay was determined by reference to the linear portion of the standard curves for FGF21 and GDF15. All assays were performed by a trained scientist or technical staff.

2.6. Statistical analysis

Statistical analyses were performed by using IBM SPSS statistics (IBM, Armonk, NY, USA). We used the nonparametric Mann–Whitney *U* test to validate differences in cytokine levels in serum between mitochondrial disease patients and controls. The correlation between GDF15 and FGF21 concentrations in serum was assessed by Spearman correlation analysis. We plotted the receiver operating characteristics (ROC) curve for GDF15, HGF, SCF, SCGF-β, and FGF21 and calculated the area under the curve (AUC). The data for the sensitivity and 100 minus the specificity were plotted on a continuous scale.

3. Results

3.1. Gene expression changes in response to intracellular energy deficiency in 2SD cells

We performed microarray analysis of 2SD cybrid cells harboring the MELAS mutation (m.3243A > G) and 2SA control cybrid cells treated with 10 mM lactate or 10 mM pyruvate for 0, 4 or 8 h (Fig. 1A). The numbers of gene probes whose signal intensities were altered by 2-fold for each comparison are given in Supplementary Tables 3–6. We found remarkable changes in gene expression in 2SD cells, but not in 2SA cells, treated with lactate for 8 h. As shown in Supplementary Fig. 1A, we then selected gene probes that were increased by lactate treatment for 8 h compared with those without treatment and concurrently up-regulated by lactate but not by pyruvate at 8 h after treatment and thereby identified 313 probes that were specifically up-regulated by lactate in 2SD cells at 8 h

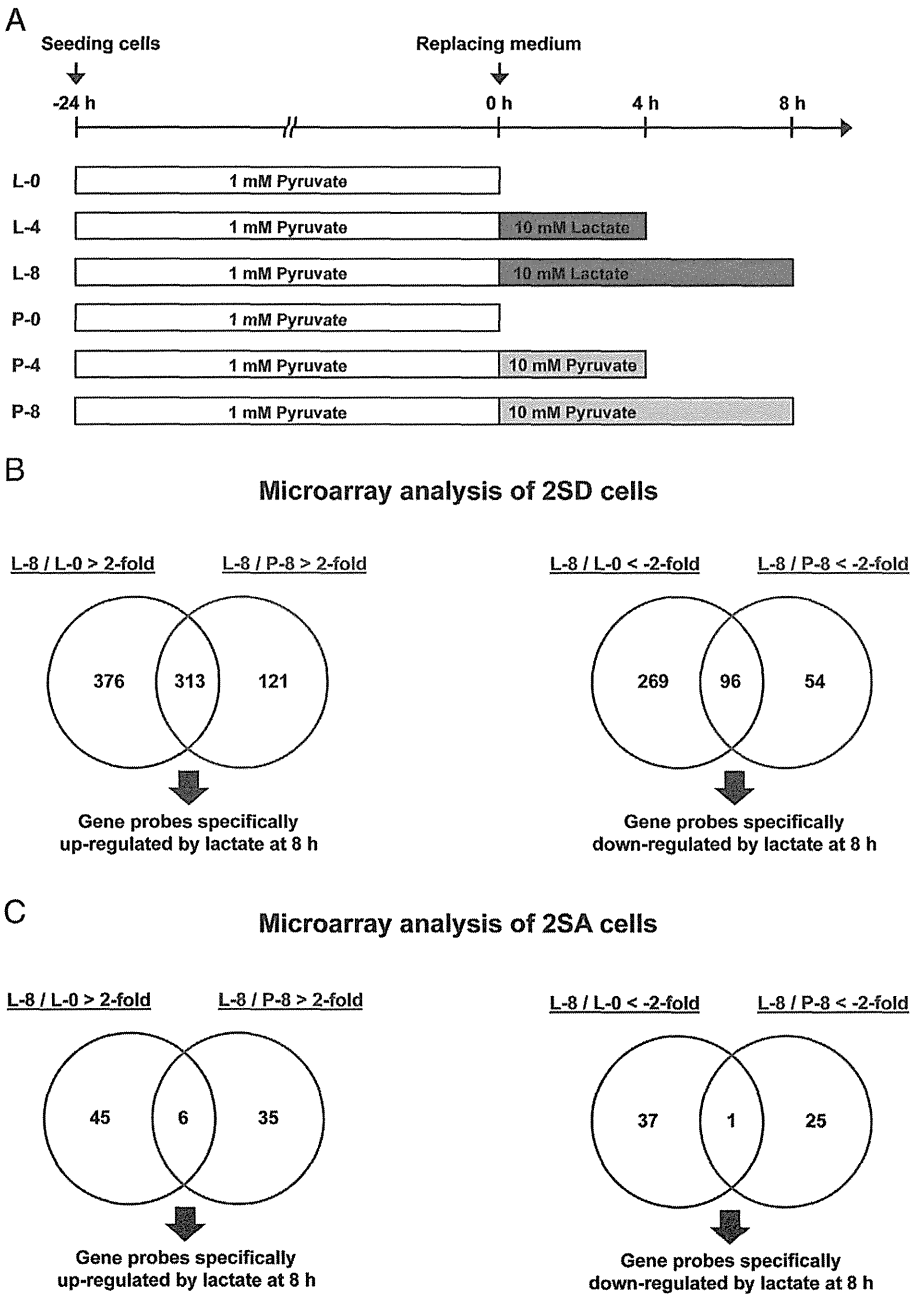

Fig. 1. Microarray analysis of 2SD and 2SA cells (A) Diagram of treatment protocols. Total RNA isolated from 2SD and 2SA cells treated with 10 mM lactate or 10 mM pyruvate for 0, 4, or 8 h were subjected to microarray analysis ($n = 2$). (B, C) Venn diagrams show the number of probes for genes in 2SD cells (B) or 2SA cells (C) that were increased (left panels) or decreased (right panels) in expression by lactate treatment for 8 h compared with their expression at 0 h and concurrently up-regulated by lactate but not by pyruvate after 8-h treatment. (For interpretation of the references to colour in this figure, the reader is referred to the web version of this article.)

(Fig. 1B). Using similar criteria (Supplementary Fig. 1B), we also identified 96 probes that were specifically down-regulated in 2SD cells by lactate treatment for 8 h (Fig. 1B). In 2SA cells, having normal mitochondrial function, the numbers of gene probes that responded to lactate treatment were limited (Fig. 1C). The clustering analysis of the 313 up-regulated (corresponding to 231 genes) and 96 down-regulated (corresponding to 75 genes) gene probes highlighted significant differences in gene expression patterns between 2SD and 2SA cells and also between lactate and pyruvate treatments (Fig. 2). These results suggest that a defective energy metabolism caused by exposure to a high dose of lactate resulted in significant changes in gene expression in 2SD cells.

3.2. Gene networks associated with intracellular energy deficiency in 2SD cells

In order to identify gene networks associated with a defective energy metabolism in the lactate-treated 2SD cells, a gene network analysis was performed on 231 up-regulated genes and 75 down-regulated ones. This analysis identified 11 and 5 gene networks for up- and down-regulated genes, respectively (Fig. 3 and Supplementary Figs. 2 and 3). The top-ranked gene network identified for the up-regulated genes contained those related to the amino-acid starvation response, such as ASNS, ATF3, NUPR1, DDIT3, CTH, TRIB3, STC2, and PCK2 (Fig. 3A). It is worth noting that GDF15, on which we focused in the

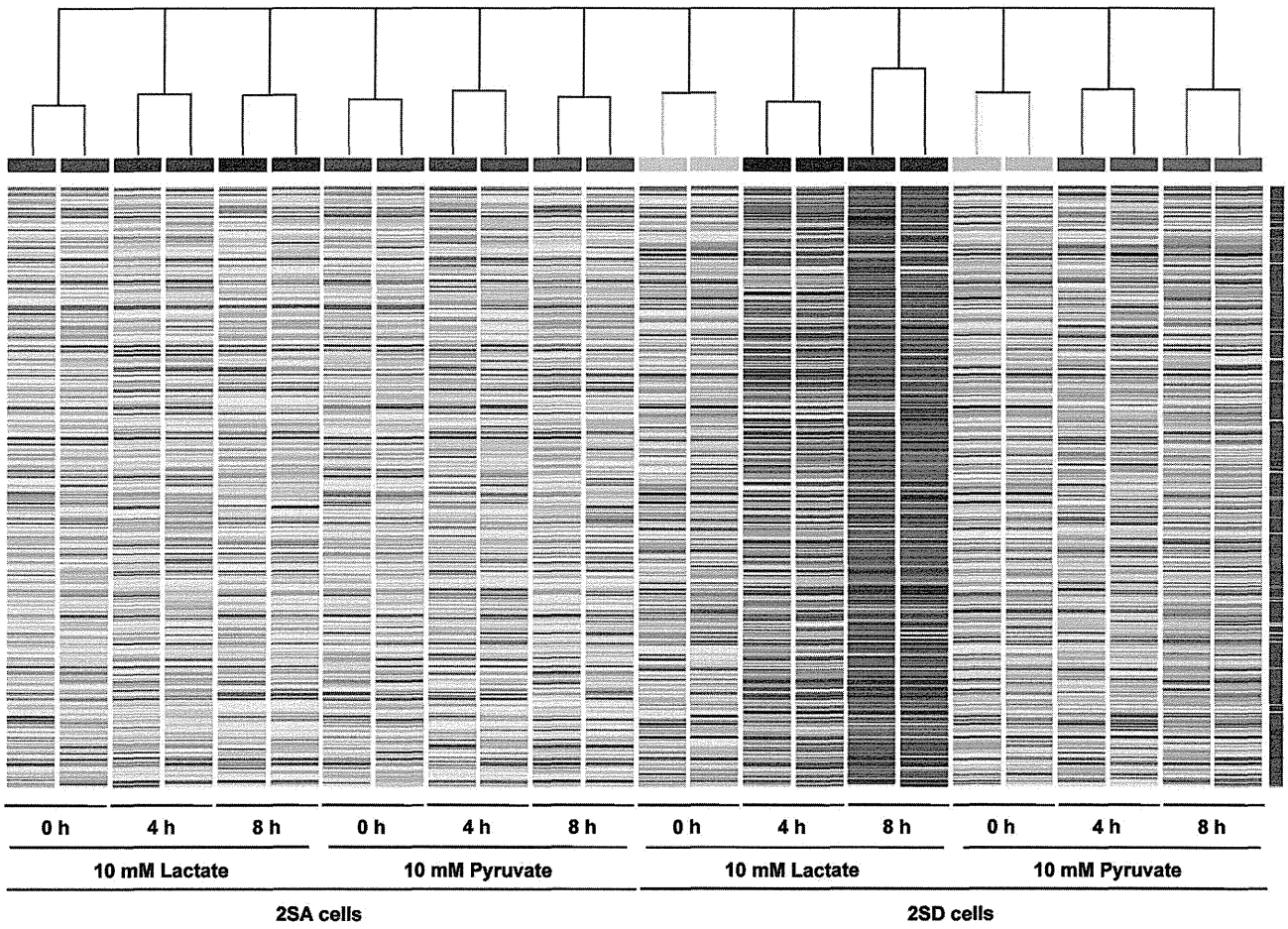

Fig. 2. Clustering analysis of the microarray data The gene probes up-regulated ($n = 313$) and down-regulated ($n = 96$) at 8 h after lactate treatment were subjected to clustering analysis. Part of the data are shown. (For interpretation of the references to colour in this figure, the reader is referred to the web version of this article.)

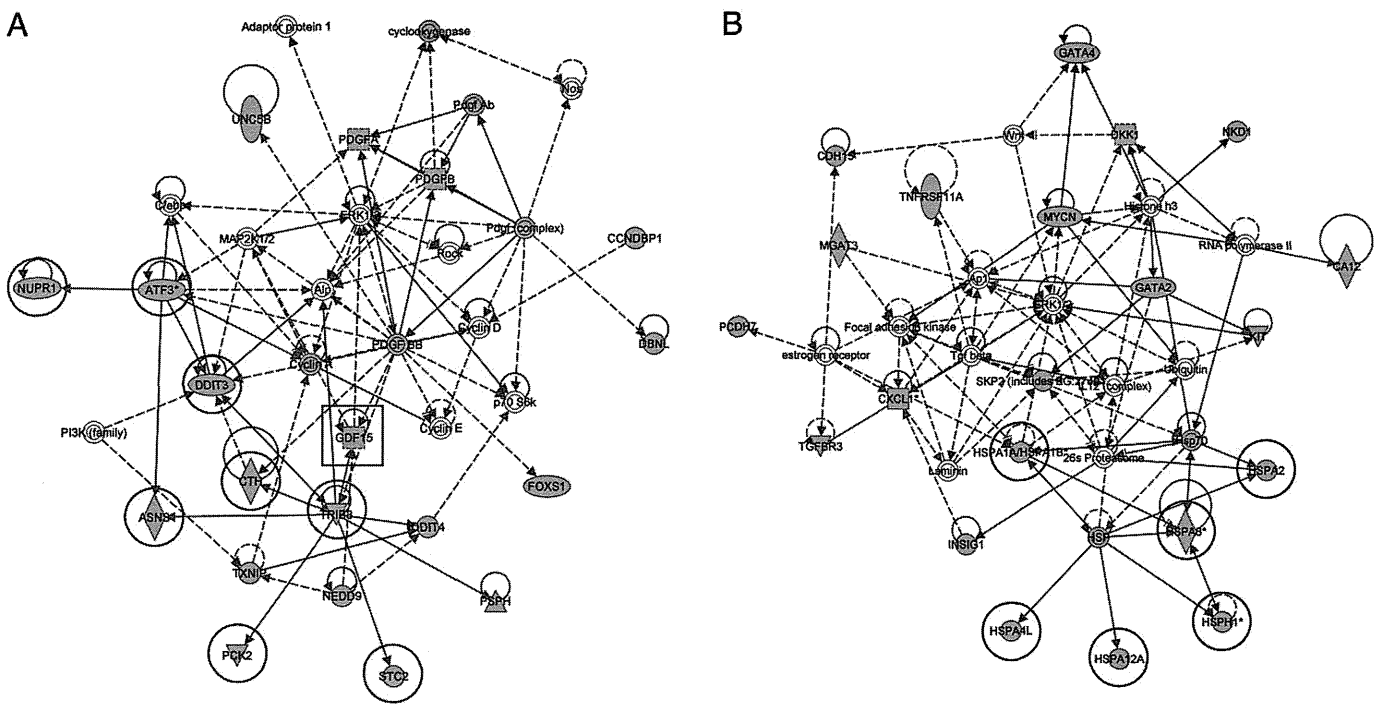

Fig. 3. Gene network analysis of the microarray data The genes specifically up-regulated ($n = 231$) and down-regulated ($n = 75$) at 8 h after lactate treatment were subjected to gene network analysis. The top-ranked gene networks in terms of the number of genes included are shown for up-regulated (A) and down-regulated (B) genes. Genes involved in the amino-acid starvation response (red circles) and heat-shock response (blue circles) as well as GDF15 (red square) are denoted. (For interpretation of the references to colour in this figure, the reader is referred to the web version of this article.)

present study, was included in this network. On the other hand, the gene network for down-regulated genes included those linked to the heat-shock protein response, such as HSPA1A, HSPA2, HSPA4L, HSPA8, HSPA12A, and HSPH1 (Fig. 3B).

3.3. GDF15 as a potential biomarker for diagnosis and evaluating the therapeutic efficacy of pyruvate

Proteins encoded by genes related to intracellular energy deficiency in 2SD cells and secreted into the medium could be potential biomarkers for mitochondrial diseases. Gene annotation analysis revealed the location of gene products that were specifically up- and down-regulated by lactate at 8 h (231 and 75 genes, respectively) (Table 1). Twenty-three up-regulated genes and 4 down-regulated genes were annotated to the extracellular space, each of which is listed in Tables 2 and 3. Among them, we focused on the top 2 ranked up-regulated genes, growth differentiation factor 15 (GDF15) and inhibin beta E (INHBE).

To validate the intracellular expression levels of these genes, we performed quantitative RT-PCR for GDF15 and INHBE. The expression levels of GDF15 (Fig. 4A) and INHBE (Fig. 4B) in the 2SD cells were increased by treatment with 10 mM lactate, but not with 10 mM pyruvate, for 4 or 8 h. Furthermore, GDF15 expression at 0 h was higher in 2SD cells than in 2SA cells. These results confirmed the reproducibility of our microarray data and identified GDF15 and INHBE as candidate biomarkers. To determine whether the secretion of GDF15 and INHBE proteins was increased in 2SD cells in response to lactate treatment, we measured their concentrations in medium from 2SA and 2SD cells cultured for 24 h in the presence of 1 mM pyruvate, 10 mM lactate, or 10 mM pyruvate. ELISA showed that the GDF15 levels were higher in the conditioned medium of 2SD cells than in that of 2SA cells under all of the culture conditions (Fig. 4C). Moreover, treatment with 10 mM lactate, but not with 10 mM pyruvate, promoted secretion of GDF15 in 2SD cells in comparison with treatment with 1 mM pyruvate, whereas 2SA cells did not respond to the high dose of lactate and pyruvate treatment. In contrast, INHBE protein was not detectable by ELISA in the conditioned medium of either 2SD or 2SA cells under any culture conditions (data not shown). These results indicate that GDF15 could be a potential biomarker for diagnosis and monitoring the disease status and progression as well as for assessing the therapeutic efficacy of pyruvate for the treatment of mitochondrial diseases.

3.4. GDF15 as a biomarker for diagnosis of mitochondrial diseases

In order to validate the feasibility of GDF15 as a serum biomarker, we measured its concentration in the serum of 17 patients with mitochondrial diseases as well as in that of 13 patients with other pediatric diseases as a control (Supplementary Table 2). ELISA showed that the average concentration of GDF15 in the serum of mitochondrial disease patients was 2632.9 pg/mL, whereas that for other pediatric disease patients was 285.2 pg/mL, suggesting that GDF15 levels were significantly increased in the serum of mitochondrial disease patients and could clearly distinguish mitochondrial disease patients from control patients (Fig. 5A).

Table 1
The location of probes (genes) up- and down-regulated in 2SD cells with lactate treatment for 8 h.

Location	Up-regulated		Down-regulated	
	Probe number	Gene number	Probe number	Gene number
Nucleus	39	35	14	14
Cytoplasm	51	47	25	19
Plasma membrane	37	33	16	16
Extracellular space	26	23	5	4
Unknown	160	93	36	22

Since fibroblast growth factor 21 (FGF21) was recently proposed as a diagnostic marker for mitochondrial diseases (Davis et al., 2013; Suomalainen et al., 2011), we also measured the FGF21 levels in the serum of the same mitochondrial disease patients and control patients (Fig. 5B). The serum FGF21 levels were higher in patients with mitochondrial diseases than in those with other diseases. Furthermore, there was a good correlation between the serum GDF15 and FGF21 levels (Fig. 5C).

In an attempt to find additional biomarkers, we determined the serum levels of 21 cytokines in the same patients by using the multiplex suspension array. As shown in Supplementary Fig. 4A, the serum concentrations of HGF and SCF were higher in patients with mitochondrial diseases than in control patients, whereas the serum levels of SCGF-β were lower in the former than in the latter.

Finally, we performed ROC curve analysis of GDF15, HGF, SCF, SCGF-β, and FGF21. As shown in Fig. 5D, the area under the curves (AUC) for GDF15 (0.986) was higher than that for FGF21 (0.787). The AUC for FGF21 was similar to those for HGF (0.747), SCF (0.729), and SCGF-β (0.837) (Supplementary Fig. 4B), indicating that GDF15 had the maximum sensitivity and specificity for diagnosis of mitochondrial diseases. These results suggest that GDF15 has the greatest potential as a novel diagnostic marker for MELAS and other mitochondrial diseases.

4. Discussion

Based on the global gene expression analysis of cybrid cells with mitochondrial dysfunction, we identified GDF15 as a potential biomarker whose expression and secretion reflected the intracellular energy deficiency and the effect of pyruvate therapy on the energy metabolism. We then determined the serum levels of GDF15 in patients with mitochondrial diseases and other diseases and identified GDF15 as a novel diagnostic marker for mitochondrial diseases. Although additional clinical studies are needed, the serum GDF15 concentration may be a useful biomarker not only for diagnosis of mitochondrial diseases but also for monitoring the disease status and progression as well as for determining the efficacy of pyruvate therapy.

GDF15 is a member of the transforming growth factor-β (TGF-β) superfamily and is widely expressed in mammalian tissues (Unsicker et al., 2013). GDF15 plays important roles in multiple pathologies including cardiovascular diseases, cancer, and inflammation. It has been shown that GDF15 is up-regulated by tumor suppressor p53 in response to high glucose or treatment with anti-cancer compounds (Baek et al., 2002; Li et al., 2013; Yang et al., 2003). The p53 protein is a transcription factor that responds to a variety of stresses such as DNA damage, oxidative stress, hypoxia, and metabolic stress, and it activates the expression of genes to induce cell cycle arrest, DNA repair, senescence, and cell death (Sermeus and Michiels, 2011; Sperka et al., 2012; Zhang et al., 2010). CDKN1A (p21), a potent cyclin-dependent kinase inhibitor, is a major downstream effector of p53, which induces cell-cycle arrest (Sperka et al., 2012). In our microarray data, the CDKN1A expression level was 3.5-fold increased by lactate treatment of 2SD cells (data not shown). Previous reports demonstrated increased expression of CDKN1A in the skeletal muscle of patients with mitochondrial diseases and a cell line depleted of mitochondrial DNA (Behan et al., 2005; Crimi et al., 2005). Besides CDKN1A, we found other p53 effector genes in the list of genes up-regulated in the lactate-treated 2SD cells, including GADD45A, EGR2, DDIT3, CHMP4C, SESN2, ULBP1, DDIT4, and NUPR1 (data not shown). These results suggest that p53 activation may have played an important role in the induction of GDF15 expression in 2SD cells treated with lactate. It has been also demonstrated that p53 activation caused by metabolic stress is mediated by AMP-activated protein kinase (AMPK; Zhang et al., 2010). Our previous metabolomic profiling revealed that the ATP level drops but that the ADP and AMP levels are increased in lactate-treated 2SD cells (Kami et al., 2012), implying that elevation of the AMP/ATP ratio may activate p53 through AMPK activation. Taken together, it is possible that p53 induced GDF15 expression in

Table 2
Genes annotated to the extracellular space among those specifically up-regulated by lactate treatment for 8 h.

Gene symbol	Accession number	Entrez gene name	Fold change	
			L-8/L-0[a]	L-8/P-8[b]
GDF15	NM_004864	Growth differentiation factor 15	27.4	14.8
INHBE	NM_031479	Inhibin, beta E	15.0	9.4
AREG	NM_001657	Amphiregulin	14.0	2.2
ECM2	NM_001393	Extracellular matrix protein 2, female organ and adipocyte specific	11.8	9.0
ADM2	NM_024866	Adrenomedullin 2	10.3	3.0
MMP3	NM_002422	Matrix metallopeptidase 3 (stromelysin 1, progelatinase)	9.8	4.2
IL1A	NM_000575	Interleukin 1, alpha	7.6	6.0
C12orf39	ENST00000256969	Chromosome 12 open reading frame 39	6.3	6.7
APOL6	NM_030641	Apolipoprotein L, 6	6.2	3.8
SCG5	NM_003020	Secretogranin V (7B2 protein)	5.2	3.0
SPOCK2	NM_014767	Sparc/osteonectin, cwcv and kazal-like domains proteoglycan (testican) 2	5.1	6.6
AMTN	NM_212557	Amelotin	5.0	3.9
IL23A	NM_016584	Interleukin 23, alpha subunit p19	4.4	2.8
ADAMTS17	NM_139057	ADAM metallopeptidase with thrombospondin type 1 motif, 17	3.5	2.2
VEGFA	NM_001025370	Vascular endothelial growth factor A	3.4	2.5
STC2	NM_003714	Stanniocalcin 2	3.4	2.6
PDGFB	NM_002608	Platelet-derived growth factor beta polypeptide	2.8	3.8
C1QTNF1	NM_198594	C1q and tumor necrosis factor related protein 1	2.6	2.9
HECW2	NM_020760	HECT, C2 and WW domain containing E3 ubiquitin protein ligase 2	2.4	2.1
IGFALS	NM_004970	Insulin-like growth factor binding protein, acid labile subunit	2.3	2.5
IGFBP1	NM_000596	Insulin-like growth factor binding protein 1	2.3	2.1
PDGFA	NM_002607	Platelet-derived growth factor alpha polypeptide	2.2	2.2
CLEC3B	NM_003278	C-type lectin domain family 3, member B	2.1	2.2

[a]Fold change between 8 h and 0 h after lactate treatment
[b]Fold change between lactate treatment and pyruvate treatment at 8 h

response to AMPK activation caused by the intracellular energy deficiency. However, it remains to be determined whether other stresses such as oxidative stress may also have participated in p53 activation and GDF15 induction in the lactate-treated 2SD cells.

Gene network analysis demonstrated that the top-ranked network contained not only genes associated with the amino-acid starvation response but also the GDF15 gene (Fig. 3A). In a mouse model of late-onset mitochondrial myopathy, the expression of amino-acid starvation-responsive genes was shown to be elevated (Tyynismaa et al., 2010). The asparagine synthetase (ASNS), which is a representative gene involved in the amino-acid starvation response, has been reported to be up-regulated in the skeletal muscle of patients with mitochondrial diseases and in cybrid cells established from a mitochondrial disease patient (Crimi et al., 2005; Fujita et al., 2007). Activating transcription factor 4 (ATF4) is a master regulator of integrated stress responses (ISR), in which a variety of stresses, including amino-acid starvation as well as glucose starvation, ER stress, hypoxia, and oxidative stress, induce phosphorylation of eIF2α followed by up-regulation of ATF4 to activate expression of stress-responsive genes (Harding et al., 2003; Jiang et al., 2004; Rouschop et al., 2010; Rzymski et al., 2010; Teske et al., 2011). It is noteworthy to point out that GDF15 has been shown to be up-regulated by ATF4 in mouse embryonic fibroblasts (Jousse et al., 2007). Taken together, such findings suggest that the ISR pathway may also contribute to the induction of GDF15 in response to defective energy metabolism and play a role in the pathogenesis of mitochondrial diseases.

In the present study, we validated the clinical usefulness of GDF15 as a diagnostic marker by determining the serum GDF15 levels in patients with mitochondrial diseases and in those with other pediatric diseases. The results showed that serum GDF15 levels were significantly elevated in patients with mitochondrial diseases, which finding is consistent with a recent report (Kalko et al., 2014). We also demonstrated that GDF15 had higher sensitivity and specificity than FGF21, which was recently identified as a sensitive and specific blood biomarker for muscle pathology in a wide range of mitochondrial diseases in adults and children (Suomalainen et al., 2011). Our small-scale study, however, may have underestimated the clinical usefulness of FGF21, because the AUC for FGF21 reported by 2 independent groups (0.95 and 0.91) was higher than that in the present study (0.787).

Using the multiplex suspension array, we also identified HGF, SCF, and SCGF-β as potential diagnostic markers for mitochondrial diseases. The ROC curve analysis, however, revealed that GDF15 had the maximum sensitivity and specificity for diagnosis of mitochondrial diseases compared with HGF, SCF, SCGF-β, or FGF21. Based on the microarray analysis, we also selected INHBE as the next best candidate gene (Table 2). INHBE is a member of the activin beta family, which has been reported to be primarily expressed in the liver and up-regulated by drug-induced ER stress, cysteine deprivation, and insulin treatment (Bruning et al., 2012; Dombroski et al., 2010; Hashimoto et al., 2009; Lee et al., 2008). Although secreted INHBE protein was not detectable in the conditioned medium from the cell cultures, we are currently investigating the clinical usefulness of INHBE as a biomarker for diagnosis and monitoring of the disease status and progression.

Table 3
Genes annotated to the extracellular space among those specifically down-regulated by lactate treatment for 8 h.

Gene symbol	Accession number	Entrez gene name	Fold change	
			L-8/L-0[a]	L-8/P-8[b]
CXCL1	NM_001511	Chemokine (C-X-C motif) ligand 1 (melanoma growth stimulating activity, alpha)	−3.4	−2.6
PDZRN3	NM_015009	PDZ domain containing ring finger 3	−2.4	−2.0
SLC39A10	NM_020342	Solute carrier family 39 (zinc transporter), member 10	−2.3	−2.9
DKK1	NM_012242	Dickkopf 1 homolog (Xenopus laevis)	−2.1	−2.3

[a]Fold change between 8 h and 0 h after lactate treatment
[b]Fold change between lactate treatment and pyruvate treatment at 8 h

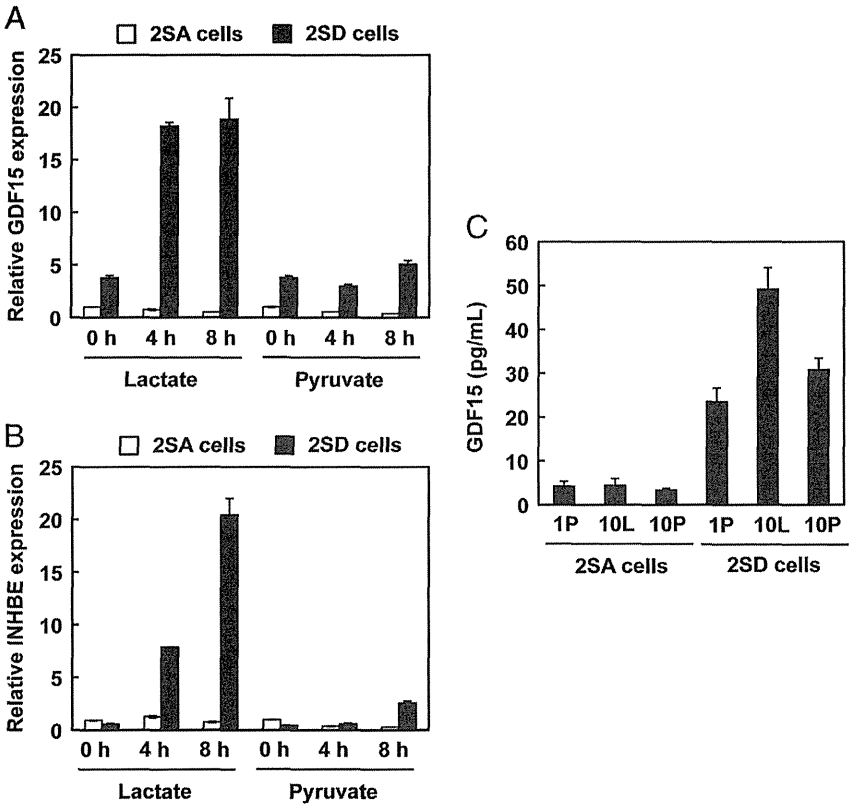

Fig. 4. Quantitative RT-PCR and ELISA for GDF15 and INHBE Total RNA isolated from 2SA and 2SD cells treated with 10 mM lactate or 10 mM pyruvate for 0, 4 or 8 h (n = 3) were subjected to quantitative RT-PCR for GDF15 (A) and INHBE (B). (C) The conditioned medium collected from 2SA and 2SD cell cultures treated with 10 mM lactate (10 L), 10 mM pyruvate (10P) or 1 mM pyruvate (1P) for 24 h was subjected to ELISA for GDF15 protein ($n = 3$).

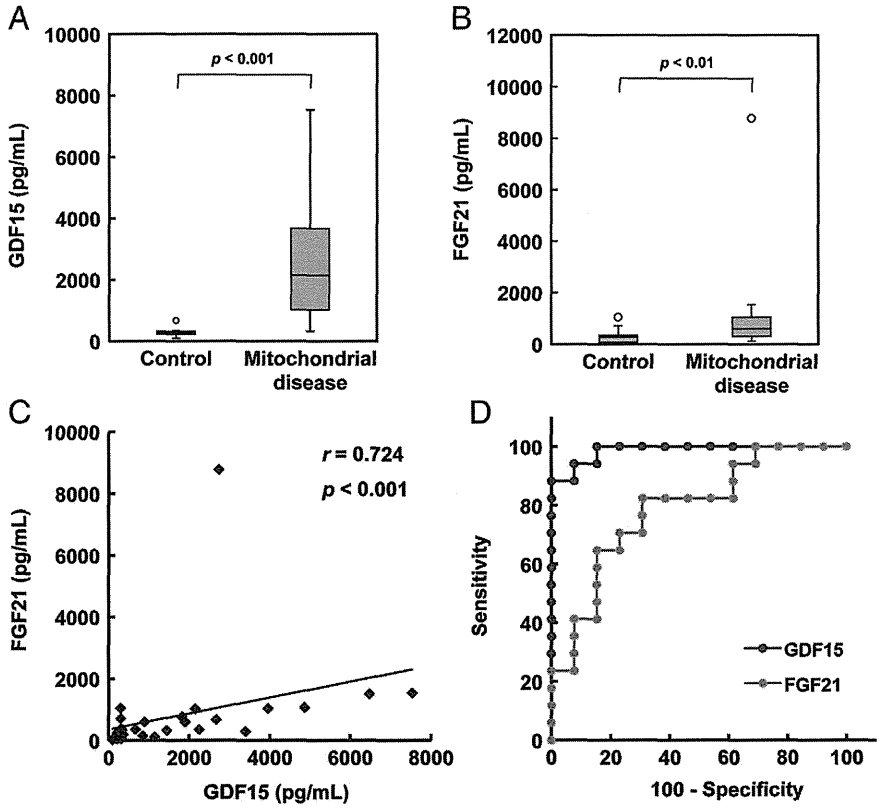

Fig. 5. Measurement of the GDF15 and FGF21 concentrations in the serum of patients. The serum GDF15 (A) and FGF21 (B) concentrations in 17 patients with mitochondrial diseases as well as those in 13 patients with other pediatric diseases were determined by ELISA. The outlier is shown with an open symbol. (C) A correlation analysis between the serum GDF15 and FGF21 levels was performed for the patients described above by use of IBM SPSS statistics. (D) The ROC curve analysis for GDF15 and FGF21 was performed. Areas under the curves (AUC) for GDF15 and FGF21 were 0.986 (95% CI 0.957-1.000) and 0.787 (95% CI 0.621-0.953), respectively.

It is well known that mitochondrial dysfunction is associated with the pathology of various diseases such as Parkinson's disease, Alzheimer's disease, diabetes, and aging (Exner et al., 2012; Lopez-Otin et al., 2013; Martin and McGee, 2014). GDF15, which may reflect mitochondria dysfunction, could be a useful marker for those diseases and the aging process. In support of this idea, the serum GDF15 level was reported to be elevated under various pathological conditions such as cancers, cardiovascular diseases, diabetes, and obesity (Dostalova et al., 2009; Kempf et al., 2007; Welsh et al., 2003); however, in most cases, it was not as high as that observed in mitochondrial diseases. Recent cohort studies also demonstrated that the serum GDF15 level is a novel predictor of all-cause mortality and is associated with cognitive performance and cognitive decline (Fuchs et al., 2013; Wiklund et al., 2010). We thus anticipate that GDF15 will attract more interest with respect to a variety of diseases and aging associated with mitochondrial dysfunction.

In conclusion, we identified GDF15 as a novel serum marker for the diagnosis of mitochondrial diseases and possibly both for monitoring the disease status and progression and for evaluating the therapeutic efficacy of pyruvate. Large-scale clinical trials including combined use of other markers such as FGF21 should confirm the clinical usefulness of GDF15.

Acknowledgments

This study was supported in part by the Ministry of Education, Culture, Sports, Science, and Technology of Japan; GMEXT/JSPS KAKENHI Grant Number: A-25242062, A-22240072, B-21390459, C-26670481, C-21590411, CER-24650414 (to M.T.), C-26350922 (to Y.F.), C-25461571 (to Y.K.), and YSB-25860891 (to S.Y.); the Ministry of Health, Labor, and Welfare of Japan; Grants-in-Aid for Research on Intractable Diseases (Mitochondrial Disorders): 23-Nanchi-Ippan-016, 23-Nanchi-Ippan-116, and 24-Nanchi-Ippan-005 (to M.T., and Y.K.); and the Takeda Science Foundation (to M.T.).

Appendix A. Supplementary data

Supplementary data to this article can be found online at http://dx.doi.org/10.1016/j.mito.2014.10.006.

References

Baek, S.J., Wilson, L.C., Eling, T.E., 2002. Resveratrol enhances the expression of non-steroidal anti-inflammatory drug-activated gene (NAG-1) by increasing the expression of p53. Carcinogenesis 23, 425–434.

Behan, A., Doyle, S., Farrell, M., 2005. Adaptive responses to mitochondrial dysfunction in the rho degrees Namalwa cell. Mitochondrion 5, 173–193.

Bruning, A., Matsingou, C., Brem, G.J., Rahmeh, M., Mylonas, I., 2012. Inhibin beta E is upregulated by drug-induced endoplasmic reticulum stress as a transcriptional target gene of ATF4. Toxicol. Appl. Pharmacol. 264, 300–304.

Chomyn, A., Martinuzzi, A., Yoneda, M., Daga, A., Hurko, O., Johns, D., Lai, S.T., Nonaka, I., Angelini, C., Attardi, G., 1992. MELAS mutation in mtDNA binding site for transcription termination factor causes defects in protein synthesis and in respiration but no change in levels of upstream and downstream mature transcripts. Proc. Natl. Acad. Sci. U. S. A. 89, 4221–4225.

Crimi, M., Bordoni, A., Menozzi, G., Riva, L., Fortunato, F., Galbiati, S., Del Bo, R., Pozzoli, U., Bresolin, N., Comi, G.P., 2005. Skeletal muscle gene expression profiling in mitochondrial disorders. Faseb J. 19, 866–868.

Davis, R.L., Liang, C., Edema-Hildebrand, F., Riley, C., Needham, M., Sue, C.M., 2013. Fibroblast growth factor 21 is a sensitive biomarker of mitochondrial disease. Neurology 81, 1819–1826.

Dombroski, B.A., Nayak, R.R., Ewens, K.G., Ankener, W., Cheung, V.G., Spielman, R.S., 2010. Gene expression and genetic variation in response to endoplasmic reticulum stress in human cells. Am. J. Hum. Genet. 86, 719–729.

Dostalova, I., Roubicek, T., Bartlova, M., Mraz, M., Lacinova, Z., Haluzikova, D., Kavalkova, P., Matoulek, M., Kasalicky, M., Haluzik, M., 2009. Increased serum concentrations of macrophage inhibitory cytokine-1 in patients with obesity and type 2 diabetes mellitus: the influence of very low calorie diet. Eur. J. Endocrinol. 161, 397–404.

Exner, N., Lutz, A.K., Haass, C., Winklhofer, K.F., 2012. Mitochondrial dysfunction in Parkinson's disease: molecular mechanisms and pathophysiological consequences. EMBO J. 31, 3038–3062.

Fuchs, T., Trollor, J.N., Crawford, J., Brown, D.A., Baune, B.T., Samaras, K., Campbell, L., Breit, S.N., Brodaty, H., Sachdev, P., Smith, E., 2013. Macrophage inhibitory cytokine-1 is associated with cognitive impairment and predicts cognitive decline - the Sydney Memory and Aging Study. Aging Cell 12, 882–889.

Fujita, Y., Ito, M., Nozawa, Y., Yoneda, M., Oshida, Y., Tanaka, M., 2007. CHOP (C/EBP homologous protein) and ASNS (asparagine synthetase) induction in cybrid cells harboring MELAS and NARP mitochondrial DNA mutations. Mitochondrion 7, 80–88.

Goto, Y., Nonaka, I., Horai, S., 1990. A mutation in the tRNA(Leu)(UUR) gene associated with the MELAS subgroup of mitochondrial encephalomyopathies. Nature 348, 651–653.

Goto, Y., Horai, S., Matsuoka, T., Koga, Y., Nihei, K., Kobayashi, M., Nonaka, I., 1992. Mitochondrial myopathy, encephalopathy, lactic acidosis, and stroke-like episodes (MELAS): a correlative study of the clinical features and mitochondrial DNA mutation. Neurology 42, 545–550.

Harding, H.P., Zhang, Y., Zeng, H., Novoa, I., Lu, P.D., Calfon, M., Sadri, N., Yun, C., Popko, B., Paules, R., Stojdl, D.F., Bell, J.C., Hettmann, T., Leiden, J.M., Ron, D., 2003. An integrated stress response regulates amino acid metabolism and resistance to oxidative stress. Mol. Cell 11, 619–633.

Hashimoto, O., Sekiyama, K., Matsuo, T., Hasegawa, Y., 2009. Implication of activin E in glucose metabolism: transcriptional regulation of the inhibin/activin betaE subunit gene in the liver. Life Sci. 85, 534–540.

Jiang, H.Y., Wek, S.A., McGrath, B.C., Lu, D., Hai, T., Harding, H.P., Wang, X., Ron, D., Cavener, D.R., Wek, R.C., 2004. Activating transcription factor 3 is integral to the eukaryotic initiation factor 2 kinase stress response. Mol. Cell. Biol. 24, 1365–1377.

Jousse, C., Deval, C., Maurin, A.C., Parry, L., Cherasse, Y., Chaveroux, C., Lefloch, R., Lenormand, P., Bruhat, A., Fafournoux, P., 2007. TRB3 inhibits the transcriptional activation of stress-regulated genes by a negative feedback on the ATF4 pathway. J. Biol. Chem. 282, 15851–15861.

Kalko, S.G., Paco, S., Jou, C., Rodriguez, M.A., Meznaric, M., Rogac, M., Jekovec-Vrhovsek, M., Sciacco, M., Moggio, M., Fagiolari, G., De Paepe, B., De Meirleir, L., Ferrer, I., Roig-Quilis, M., Munell, F., Montoya, J., Lopez-Gallardo, E., Ruiz-Pesini, E., Artuch, R., Montero, R., Torner, F., Nascimento, A., Ortez, C., Colomer, J., Jimenez-Mallebrera, C., 2014. Transcriptomic profiling of TK2 deficient human skeletal muscle suggests a role for the p53 signalling pathway and identifies growth and differentiation factor-15 as a potential novel biomarker for mitochondrial myopathies. BMC Genomics 15, 91.

Kami, K., Fujita, Y., Igarashi, S., Koike, S., Sugawara, S., Ikeda, S., Sato, N., Ito, M., Tanaka, M., Tomita, M., Soga, T., 2012. Metabolomic profiling rationalized pyruvate efficacy in cybrid cells harboring MELAS mitochondrial DNA mutations. Mitochondrion 12, 644–653.

Kempf, T., Horn-Wichmann, R., Brabant, G., Peter, T., Allhoff, T., Klein, G., Drexler, H., Johnston, N., Wallentin, L., Wollert, K.C., 2007. Circulating concentrations of growth-differentiation factor 15 in apparently healthy elderly individuals and patients with chronic heart failure as assessed by a new immunoradiometric sandwich assay. Clin. Chem. 53, 284–291.

Kirino, Y., Yasukawa, T., Ohta, S., Akira, S., Ishihara, K., Watanabe, K., Suzuki, T., 2004. Codon-specific translational defect caused by a wobble modification deficiency in mutant tRNA from a human mitochondrial disease. Proc. Natl. Acad. Sci. U. S. A. 101, 15070–15075.

Koga, Y., Povalko, N., Katayama, K., Kakimoto, N., Matsuishi, T., Naito, E., Tanaka, M., 2012. Beneficial effect of pyruvate therapy on Leigh syndrome due to a novel mutation in PDH E1alpha gene. Brain Dev. 34, 87–91.

Lee, J.I., Dominy Jr., J.E., Sikalidis, A.K., Hirschberger, L.L., Wang, W., Stipanuk, M.H., 2008. HepG2/C3A cells respond to cysteine deprivation by induction of the amino acid deprivation/integrated stress response pathway. Physiol. Genomics 33, 218–229.

Li, J., Yang, L., Qin, W., Zhang, G., Yuan, J., Wang, F., 2013. Adaptive induction of growth differentiation factor 15 attenuates endothelial cell apoptosis in response to high glucose stimulus. PLoS One 8, e65549.

Lopez-Otin, C., Blasco, M.A., Partridge, L., Serrano, M., Kroemer, G., 2013. The hallmarks of aging. Cell 153, 1194–1217.

Martin, S.D., McGee, S.L., 2014. The role of mitochondria in the aetiology of insulin resistance and type 2 diabetes. Biochim. Biophys. Acta 1840, 1303–1312.

Pavlakis, S.G., Phillips, P.C., DiMauro, S., De Vivo, D.C., Rowland, L.P., 1984. Mitochondrial myopathy, encephalopathy, lactic acidosis, and strokelike episodes: a distinctive clinical syndrome. Ann. Neurol. 16, 481–488.

Rouschop, K.M., van den Beucken, T., Dubois, L., Niessen, H., Bussink, J., Savelkouls, K., Keulers, T., Mujcic, H., Landuyt, W., Voncken, J.W., Lambin, P., van der Kogel, A.J., Koritzinsky, M., Wouters, B.G., 2010. The unfolded protein response protects human tumor cells during hypoxia through regulation of the autophagy genes MAP1LC3B and ATG5. J. Clin. Invest. 120, 127–141.

Rzymski, T., Milani, M., Pike, L., Buffa, F., Mellor, H.R., Winchester, L., Pires, I., Hammond, E., Ragoussis, I., Harris, A.L., 2010. Regulation of autophagy by ATF4 in response to severe hypoxia. Oncogene 29, 4424–4435.

Saito, K., Kimura, N., Oda, N., Shimomura, H., Kumada, T., Miyajima, T., Murayama, K., Tanaka, M., Fujii, T., 2012. Pyruvate therapy for mitochondrial DNA depletion syndrome. Biochim. Biophys. Acta 1820, 632–636.

Sermeus, A., Michiels, C., 2011. Reciprocal influence of the p53 and the hypoxic pathways. Cell Death Dis. 2, e164.

Sperka, T., Wang, J., Rudolph, K.L., 2012. DNA damage checkpoints in stem cells, ageing and cancer. Nat. Rev. Mol. Cell Biol. 13, 579–590.

Suomalainen, A., Elo, J.M., Pietilainen, K.H., Hakonen, A.H., Sevastianova, K., Korpela, M., Isohanni, P., Marjavaara, S.K., Tyni, T., Kiuru-Enari, S., Pihko, H., Darin, N., Ounap, K., Kluijtmans, L.A., Paetau, A., Buzkova, J., Bindoff, L.A., Annunen-Rasila, J., Uusimaa, J., Rissanen, A., Yki-Jarvinen, H., Hirano, M., Tulinius, M., Smeitink, J., Tyynismaa, H., 2011. FGF-21 as a biomarker for muscle-manifesting mitochondrial respiratory chain deficiencies: a diagnostic study. Lancet Neurol. 10, 806–818.

Tanaka, M., Nishigaki, Y., Fuku, N., Ibi, T., Sahashi, K., Koga, Y., 2007. Therapeutic potential of pyruvate therapy for mitochondrial diseases. Mitochondrion 7, 399–401.

Teske, B.F., Wek, S.A., Bunpo, P., Cundiff, J.K., McClintick, J.N., Anthony, T.G., Wek, R.C., 2011. The eIF2 kinase PERK and the integrated stress response facilitate activation of ATF6 during endoplasmic reticulum stress. Mol. Biol. Cell 22, 4390–4405.

Tyynismaa, H., Carroll, C.J., Raimundo, N., Ahola-Erkkila, S., Wenz, T., Ruhanen, H., Guse, K., Hemminki, A., Peltola-Mjosund, K.E., Tulkki, V., Oresic, M., Moraes, C.T., Pietilainen, K., Hovatta, I., Suomalainen, A., 2010. Mitochondrial myopathy induces a starvation-like response. Hum. Mol. Genet. 19, 3948–3958.

Unsicker, K., Spittau, B., Krieglstein, K., 2013. The multiple facets of the TGF-beta family cytokine growth/differentiation factor-15/macrophage inhibitory cytokine-1. Cytokine Growth Factor Rev. 24, 373–384.

Welsh, J.B., Sapinoso, L.M., Kern, S.G., Brown, D.A., Liu, T., Bauskin, A.R., Ward, R.L., Hawkins, N.J., Quinn, D.I., Russell, P.J., Sutherland, R.L., Breit, S.N., Moskaluk, C.A., Frierson Jr., H.F., Hampton, G.M., 2003. Large-scale delineation of secreted protein biomarkers overexpressed in cancer tissue and serum. Proc. Natl. Acad. Sci. U. S. A. 100, 3410–3415.

Wiklund, F.E., Bennet, A.M., Magnusson, P.K., Eriksson, U.K., Lindmark, F., Wu, L., Yaghoutyfam, N., Marquis, C.P., Stattin, P., Pedersen, N.L., Adami, H.O., Gronberg, H., Breit, S.N., Brown, D.A., 2010. Macrophage inhibitory cytokine-1 (MIC-1/GDF15): a new marker of all-cause mortality. Aging Cell 9, 1057–1064.

Yang, H., Filipovic, Z., Brown, D., Breit, S.N., Vassilev, L.T., 2003. Macrophage inhibitory cytokine-1: a novel biomarker for p53 pathway activation. Mol. Cancer Ther. 2, 1023–1029.

Yasukawa, T., Suzuki, T., Ueda, T., Ohta, S., Watanabe, K., 2000. Modification defect at anticodon wobble nucleotide of mitochondrial tRNAs(Leu)(UUR) with pathogenic mutations of mitochondrial myopathy, encephalopathy, lactic acidosis, and stroke-like episodes. J. Biol. Chem. 275, 4251–4257.

Zhang, X.D., Qin, Z.H., Wang, J., 2010. The role of p53 in cell metabolism. Acta Pharmacol. Sin. 31, 1208–1212.

Molecular Genetics and Metabolism 112 (2014) 133–138

Contents lists available at ScienceDirect

Molecular Genetics and Metabolism

journal homepage: www.elsevier.com/locate/ymgme

Efficacy of pyruvate therapy in patients with mitochondrial disease: A semi-quantitative clinical evaluation study

Tatsuya Fujii [a,*], Fumihito Nozaki [a], Keiko Saito [a,1], Anri Hayashi [a], Yutaka Nishigaki [b,2], Kei Murayama [c], Masashi Tanaka [b], Yasutoshi Koga [d], Ikuko Hiejima [a], Tomohiro Kumada [a]

[a] Department of Pediatrics, Shiga Medical Center for Children, 5-7-30 Moriyama, Shiga 524-0022, Japan
[b] Department of Genomics for Longevity and Health, Tokyo Metropolitan Institute of Gerontology, 35-2 Sakane-cho, Itabashi, Tokyo 173-0015, Japan
[c] Department of Metabolism, Chiba Children's Hospital, 579-1 Heta-cho, Midori, Chiba 266-0007, Japan
[d] Department of Pediatrics and Child Health, Kurume University Graduate School of Medicine, 67 Asahi-machi, Kurume, Fukuoka 830-0011, Japan

ARTICLE INFO

Article history:
Received 26 February 2014
Received in revised form 25 April 2014
Accepted 25 April 2014
Available online 2 May 2014

Keywords:
Pyruvate
Therapy
Mitochondrial disease
NAD^+
Lactate-to-pyruvate ratio

ABSTRACT

Background: Disorders of oxidative phosphorylation (OXPHOS) cause an increase in the NADH/NAD^+ ratio, which impairs the glycolysis pathway. Treatment with pyruvate is expected to decrease the ratio and thereby restore glycolysis. There are some case reports on the efficacy of pyruvate treatment for mitochondrial diseases. However, few of these reports assessed their results using a standardized scale.

Methods: We monitored 4 bedridden patients with OXPHOS disorders who continued therapies of 0.5–1.0 g/kg/day of sodium pyruvate for more than 12 months. The efficacies of these treatments were evaluated with the Newcastle Pediatric Mitochondrial Disease Scale and the Gross Motor Function Measure with 88 items.

Results: The ages of the patients at the treatment initiation ranged from 8–100 months. Of the 4 patients, 3 exhibited improvements within 1–3 months from the initiation of treatment. Among these 3 patients, one maintained the improvement for over 2 years. The remaining 2 regressed 3–6 months after the initiation of treatment. The blood lactate/pyruvate ratios did not correlate with the efficacy of treatment.

Conclusion: Pyruvate was effective even in bedridden patients with OXPHOS disorders, at least in the short term. Clinical trials with more patients and less severe disabilities are necessary to evaluate the long-term efficacy of this treatment. Biomarkers other than lactate and pyruvate need to be identified to biochemically monitor the efficacy of this treatment.

1. Introduction

Tanaka et al. [1] proposed that pyruvate has therapeutic potential for patients with oxidative phosphorylation (OXPHOS) disorders in which the intracellular NADH/NAD^+ ratio is increased. Such an increased ratio impairs the activity of glyceraldehyde-3-phosphate dehydrogenase (GAPDH) in the glycolysis pathway. Theoretically, with lactate dehydrogenase, pyruvate provides NAD^+ and decreases this ratio and thereby restores the activity of GAPDH, which produces ATP. Additionally, pyruvate activates pyruvate dehydrogenase and non-enzymatically eliminates hydrogen peroxide.

There are several case reports on the efficacy of pyruvate in patients with OXPHOS disorders [2–4]. However, few of these reports have evaluated the clinical outcomes using a standardized clinical assessment scale. We semi-quantitatively evaluated the efficacy of pyruvate therapy in 4 patients with OXPHOS disorders using standardized scales. This study was approved by the Ethical Committee of our institution. Written informed consent was obtained from the parents of every patient.

2. Patients and methods

2.1. Patients

Four patients who had been on pyruvate for more than 12 months were studied (Table 1). Two patients had Leigh syndrome associated with m.8993 T>G or m.9176 T>C mutations. One patient had non-specific encephalomyopathy associated with complex I and IV combined deficiency. Another patient had myopathic mitochondrial DNA depletion syndrome. All patients were bedridden, and all but one

Abbreviations: NPMDS, Newcastle Pediatric Mitochondrial Disease Scale; GMFM-88, Gross Motor Function Measure with 88 items; JMDRS, Japanese Mitochondrial Disease Rating Scale; OXPHOS, Oxidative phosphorylation; MELAS, Mitochondrial myopathy, encephalopathy, lactic acidosis and stroke-like episodes; FGF-21, Fibroblast growth factor 21.

* Corresponding author at: Department of Pediatrics, Shiga Medical Center for Children, 5-7-30 Moriyama, Moriyama-City, Shiga 524-0022, Japan.
E-mail address: tatsufu@gmail.com (T. Fujii).
[1] Present address: Department of Pediatrics, Graduate School of Medicine, Kyoto University, 54 Shogoinkawahara-cho, Sakyo, Kyoto, Kyoto 606-8507, Japan.
[2] Present address: Nishigaki Clinic & Research Laboratory, 1-177 Uchinaka, Nakagawa, Nagoya 454-0927, Japan.

http://dx.doi.org/10.1016/j.ymgme.2014.04.008
1096-7192/